Forest Research
Technical Report
Coast Forest Region
2100 Labieux Road, Nanaimo, BC, Canada, V9T 6E9, 250-751-7001

TR-036 Applications March 2007

Using stereoscopic high spatial resolution satellite imagery to assess landscape and stand level characteristics

by

Karl Kliparchuk, Denis Collins and Derek Challenger

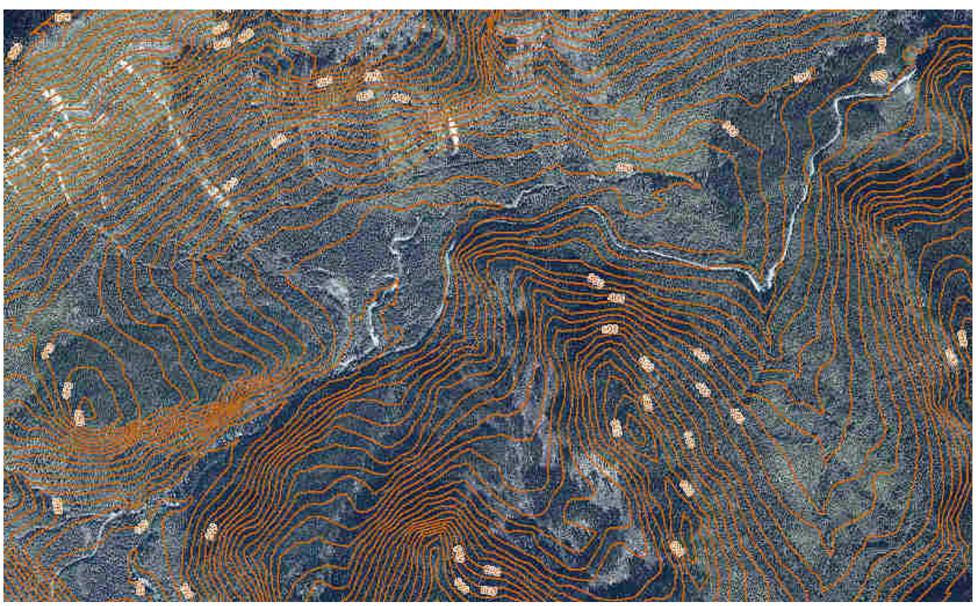

Research Disciplines: Ecology ~ Geology ~ Geomorphology ~ Hydrology ~ Pedology ~ Silviculture ~ Wildlife

Contacts:

Denis Collins, PhD, PGeo
Research and Inventory Manager
Coast Forest Region
BC Ministry of Forests and Range
2100 Labieux Road
Nanaimo, British Columbia V9T 6E9
tel. 250-751-7121
email Denis.Collins@gov.bc.ca

Karl Kliparchuk, MSc
McElhanney Consulting Services Ltd.
100 - 780 Beatty Street
Vancouver, British Columbia V6B 2M1
tel. 604-683-8521

Derek Challenger, RPF
Inventory Forester
Coast Forest Region
BC Ministry of Forests and Range
2100 Labieux Road
Nanaimo, British Columbia V9T 6E9
tel. 250-751-7133

Citation:
Kliparchuk, K., D. Collins and D. Challenger. 2007. Using stereoscopic high spatial resolution satellite imagery to assess landscape and stand level characteristics. Res. Sec., Coast For. Reg., BC Min. For., Nanaimo, BC. Tec. Rep. TR-036/2007.

website: http://www.for.gov.bc.ca/rco/research/index.htm

Cover photo: Contours derived from stereo interpretation of IKONOS imagery overlain on the image.

TABLE OF CONTENTS

Figures (continued):

SUMMARY

An ongoing remote sensing project has been under way within the Coast Forest Region since 2000. The initial parts of the project studied the uses of commercially available high spatial resolution satellite imagery for the purposes of resource feature mapping and compliance and enforcement surveillance. The Forest Practices Board, FPB/SIR/14, July 2005, made several recommendations about managing landslide risk in BC. One of the recommendations was to use high spatial resolution, multispectral data and stereoscopic viewing to improve the ability of a sensor for landslide detection. This report extends the use of high spatial resolution IKONOS imagery through the acquisition of stereo imagery and analysis of the imagery using KLT softcopy photogrammetry.

Natural colour, false colour infrared, and Principal Component Analysis images were analysed and interpreted in stereo. Due to IKONOS' large base height ratio (1 to 2), we had greater vertical exaggeration in the stereo image. This allowed the photogrammetric operator to more easily map steep slopes, and detect small variations in slope. Accuracy assessments were conducted to compare slope geometric information derived from the stereo satellite imagery with data used in TRIM maps. We determined that the elevations from the IKONOS derived Digital Elevation Model (DEM) fit closely to the TRIM DEM elevations. The mean difference was 7.3m.

We compared a natural colour RGB, a false colour near-infrared, and a Principal Components colour composite image for interpretability of forest cover features. We have concluded that an interpreter with forestry background, is more comfortable viewing the natural colour and false colour near infrared image. Neither of these colour composite images was superior for all image interpretation. We recommend that both colour composite images be used for stereo viewing and interpretation.

Some general comments on the images by the interpreter:

- Textural changes due to differences in tree heights and species can be seen, especially when changes in terrain are also evident;
- Colour differences between various tree species are not easy to distinguish compared with hard copy air photos at a similar viewing scale;
- Distinguishing individual trees by species is not easy. Neither colour variation nor crown shapes is well-defined. There is insufficient depth in viewing the tree canopies and branching patterns;
- Near-infrared does highlight age differences, especially between old growth trees on poor sites and regeneration/second growth on more productive sites. Non-vegetation features such as rock outcrops and exposed soil also stand out more;
- Generally, height measurements made on the image correlated quite well with both ocular estimates and attributes from the forest cover map, as long as the ground was visible. The more open the stand and the taller the trees, the easier it was to make accurate height measurements;
- Height measurements from the image did not correlate as well with map values where part of the original map polygon has been logged and the labels not adjusted to account for removal of the higher volume area of the stand.

Landslide volume estimates were also calculated using the softcopy photogrammetric software. This was done by capturing spot heights and break lines, to produce a DEM of the slide. We also created a hypothetical pre-slide DEM and differenced the two DEMs to calculate the volume of material removed. We also generated a slope magnitude digital landform model (DLM) from the post-slide grid.

The availability of stereoscopic high spatial resolution imagery and image analysis software that allows for digitizing in 3D greatly improves the efficiency of interpretation and identification of other geomorphic characteristics and the calculation of slope, elevation, landslide volumes and areas and other features. Recommendations regarding time of year and type of colour composite stereoscopic images to use for forest management applications are also outlined.

KEY WORDS

Remote sensing, IKONOS, effectiveness evaluation, forest resource management, stereo, photogrammetry

ACKNOWLEDGEMENTS

Funding for this project was provided by the Forest Investment Account through the Coast Forest Region of the Ministry of Forests and Range. Dr. Nicholas Coops, Remote Sensing Studio, University of British Columbia provided review comments. Thanks also to Warren Warttig of Interfor who also provided support for this project. Andrew McIntosh of McElhanney Consulting Services Ltd. provided technical support.

1.0 INTRODUCTION

Previous research in the Coast Forest Region has shown that a number of resource features are readily identifiable from high spatial resolution satellite imagery, and that remote sensing imagery has the capability to enable measurements and monitoring of change, both temporal and spatial, in distribution, condition and extent. As noted in Collins et al. (2001), the resource features of interest from an operational forest management perspective include, but are not necessarily limited to, the following:

- Landslides
- Roads
- Cutblocks, both clearcut and partial harvesting
- Vegetation types
- Stream channels and other aquatic and riparian features
- Wildlife habitat
- Coarse woody debris
- Windthrow
- Unauthorized harvesting activities

The Forest Practices Board of British Columbia conducted a

review of the effectiveness of terrain stability field assessments for minimizing landslides, and in cooperation with the Coast Forest Region and Simon Fraser University the Board utilized satellite imagery to assess landslide occurrence in harvested terrain. This project is an outcome from their report, "Managing Landslide Risk from Forest Practices in British Columbia", Forest Practices Board, FPB/SIR/14, July 2005. Some of the recommendations from this report are:

- The Ministry of Forests and Range should regularly conduct inventories of landslides as part of the Forest and Range Evaluation Program, as there is no FRPA requirement for licensees to report landslides;
- High spatial resolution, multispectral data collection, and stereoscopic viewing greatly improve the ability of a sensor for landslide detection;
- IKONOS and QUICKBIRD imagery outperformed SPOT imagery for landslide detection;
- Imagery used for landslide detection should combine three properties: high spatial resolution, multispectral data collection, and if possible, stereoscopic viewing.

Li, 1998, noted that there are several advantages to using high-spatial resolution stereo satellite imagery for photogrammetric mapping, including:

- extremely long camera focal length, for capturing terrain relief information from the satellite orbit;
- fore-, nadir-, and aft-looking linear CCD arrays supplying in-track stereo strips and "pointing" capabilities generating cross-track stereo strips; and
- a base-height (sensor baseline vs. orbit height) ratio of 0.6 and higher that is similar to aerial photographs. (For IKONOS the base-height ratio varies between 1 and 2.)

Nichol et al., 2006 investigated the use of high spatial resolution stereo satellite images for detailed landslide hazard assessment applications for large areas. They found that DEMs created from IKONOS stereo imagery appear to be more accurate and sensitive to micro-scale terrain features than those created from digital contour data. They also suggest that stereo satellite imagery is usually more cost-effective for detailed landslide hazard assessment over large areas.

We acquired stereoscopic IKONOS satellite imagery, which was loaded into a softcopy photogrammetric workstation, and the imagery was then analyzed and interpreted in three dimensions (3D stereo). The methods derived from this approach can be used by the BC Ministry of Forests and Range for inventories of landslides, and can provide knowledge on landscape and stand level characteristics which can be derived from stereoscopic, high spatial resolution satellite imagery.

2.0 METHODOLOGY

2.1 STUDY AREA

This softcopy photogrammetric analysis project was conducted on the Hesquiat/Escalante/Mooyah areas, located in and around Clayoquot Sound on the west coast of Vancouver Island (Figure 1). The area is within the South Island Forest District of the Coast Forest Region.

This area was chosen due to the significant amount of pre-existing digital and on-ground data available for it. In addition, in previous projects (Collins et al., 2001, and Collins, D and Kliparchuk, K, 2004), the authors had undertaken an analysis of the northern section of this area using high spatial resolution IKONOS and Quickbird satellite imagery.

The area's topography ranges from flat to steep-sided terrain, with elevations ranging from sea level along the coastal plain north of the Estevan Peninsula, to approximately 1,000 m elevation inland. The flats, known as the Estevan Coastal Plain, extend inland for approximately 6 km from the Escalante River mouth, and encompass the Hesquiht peninsula. Much of the area was logged in the 1960s and into the 1980s, but some recent variable retention logging has been conducted. There are numerous pre-Forest Practices Code (FPC) landslides and some natural landslides in the area (Lewis and Liard,1983), many of which were initiated during an intense storm cycle in January 1996.

The area is predominantly underlain by granitoid rocks of the Island Intrusions and Westcoast complex (Muller, 1977). Conglomerates and sandstone of the early Tertiary Escalante Group underlie part of the area, and similar lithologies of the Carmanah Group outcrop in the Hesquiat Lake area. In the North Fork of the Escalante watershed, Karmutsen Volcanics outcrop, and the bedrock is metamorphosed and intensely sheared. This, in conjunction with high rainfall and freeze-thaw processes, produces highly fractured and friable bedrock. This surficial material has resulted in the formation of deep colluvial blankets on many of the steep hillsides. Structurally controlled valleys have been glacially deepened and widened, a legacy of Quaternary glaciation. Preferential erosion along faults and other structural lineaments has eroded tributary valleys and deeply incised gully systems. Deep silty to gravelly tills, stratified gravelly glaciofluvial deposits, and laminated silts are present in the lower valley slopes.

The weather on the west coast of Vancouver Island is dominated by Pacific cyclones that cause significant cloud cover and precipitation. The area is situated within the transition between the very humid and very wet maritime Coastal Western Hemlock biogeoclimatic zones (CWHvh and CWHvm). Predominant conifer species consist of Western redcedar (*Thuja plicata*), Western hemlock (*Tsuga heterophylla*) and Amabalis fir (*Abies amabilis*). Many of the older landslides have been revegetated by red alder (*Alnus rubra*).

2.2 IKONOS SATELLITE

The IKONOS satellite was launched on September 24, 1999, as one of a new generation of satellites collecting very high spatial resolution optical image data. Orbiting at an altitude of approximately 681 km above the earth, IKONOS has a 0.82 metre resolution panchromatic sensor and a 3.2 metre resolution multispectral sensor (Table 1).

Table 1. IKONOS specifications.

Product Name	Spatial Resolution at Nadir	Spectral Bands (Micrometers)	Dynamic Range
IKONOS Multispectral	3.2 metre	Band 1: 0.445 - 0.516 (Blue) Band 2: 0.506 - 0.595 (Green) Band 3: 0.632 - 0.698 (Red) Band 4: 0.757 - 0.853 (Near Infrared)	11 Bit (2048 levels)
IKONOS Panchromatic	0.82 metre	Pan Band: 0.45 - 0.90	11 Bit (2048 levels)

GeoEye (formerly Space Imaging Inc.) of Dulles, Virginia, is the operator of the IKONOS satellite. Through a combination of different multispectral image channels, the IKONOS imagery provides a natural colour image, and a false colour infrared image that can be interpreted visually. Both the panchromatic and multispectral data from the IKONOS satellite are 11-bit, resulting in 2,048 discrete brightness levels, significantly more than traditional satellite data which are often 8-bit (for 256 levels). This increased radiometric resolution can allow greater discrimination in key regions, for example for distinguishing objects in shadow areas

IKONOS products are sold by the square kilometre of scanned area, according to customer requirements. For this project we ordered stereo satellite imagery. The satellite can point its sensor up to 60 degrees off nadir in order to capture stereo image pairs. The minimum order size is 100 sq km. The pricing for each reference colour fused panchromatic stereo pair is US $39.60/sq km. With the minimum order, each stereo pair costs US $3,960 plus shipping and taxes. (http://www.geoeye.com)

2.3 IKONOS STEREO DATA ACQUISITION

To order the Reference Stereo IKONOS imagery, latitude/longitude corner coordinates of the area of interest were provided to GeoEye. Two sets of in-track stereo images were acquired: one in the summer (Figure 2) and one in the fall (Figure 3). These two seasons were selected in order to determine if one season may provide better quality imagery, and therefore be more easily interpreted. The dates of the two Reference Stereo image pairs acquired are shown in Table 2.

The area of interest was 10x10 km in size. The images were acquired as three stereo pairs for each date, with the first two stereo pairs covering approximately 99% of the area. As each

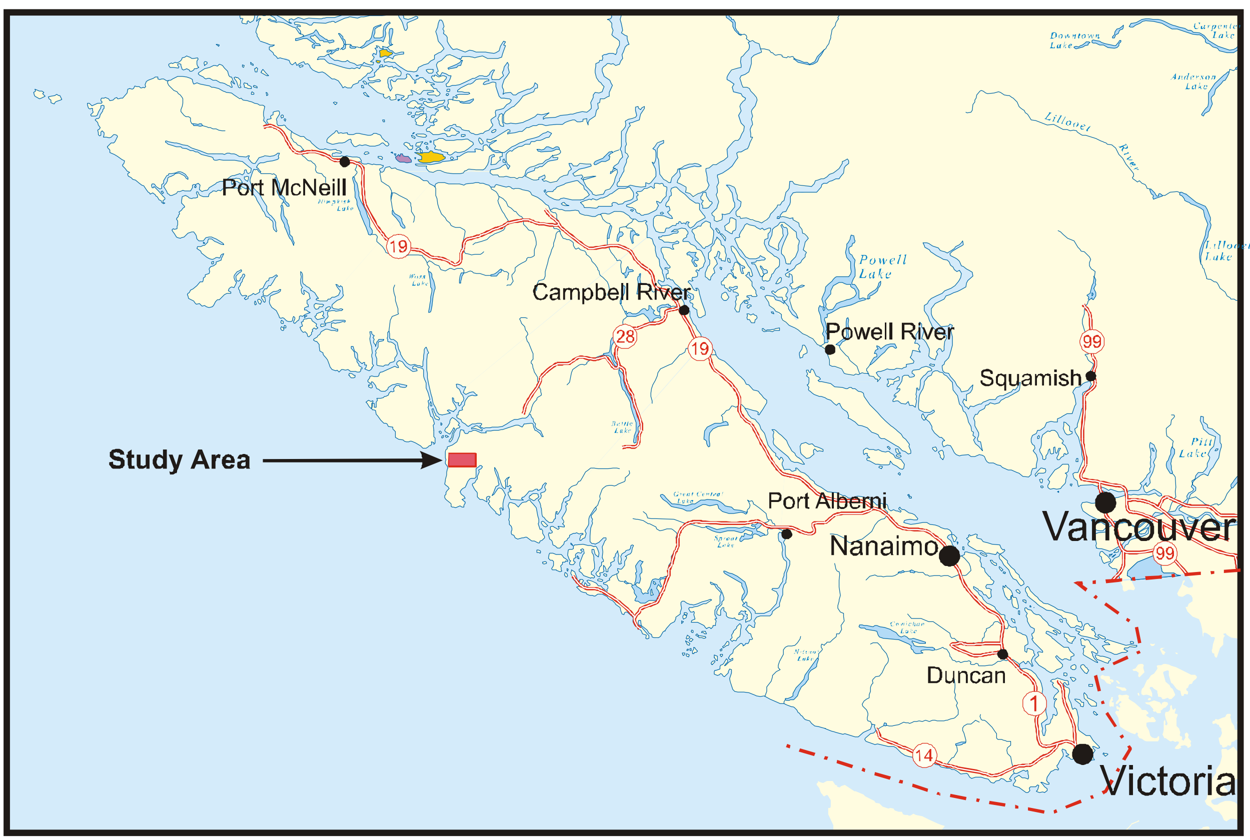

Figure 1. Study area location.

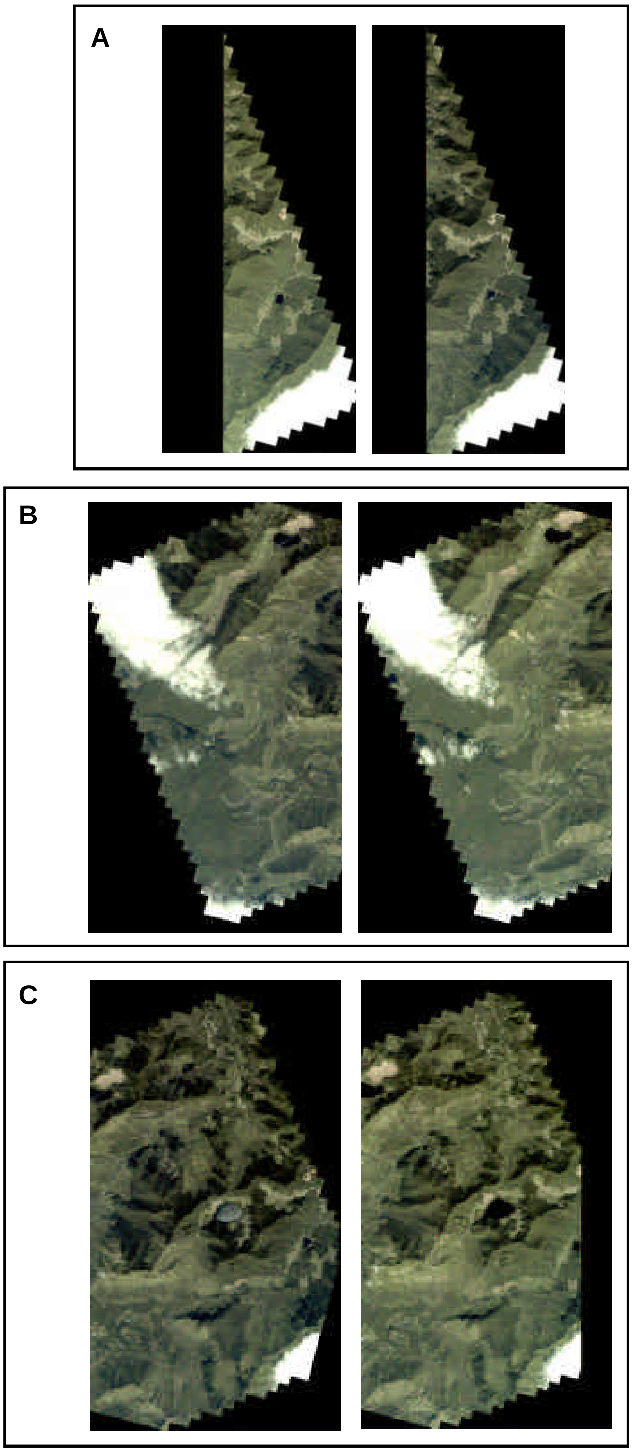

Figure 2. August 2006 IKONOS natural colour image coverage of Hesquiat / Mooyah area (stereo image pairs).

Image IDs: © GeoEye
Pair A, *left*, po_200310_rgb_0010000000_ovr.jpg, *right*, po_200310_rgb_0000010000_ovr.jpg.
Pair B, *left*, po_200310_rgb_0030020000_ovr.jpg, *right*, po_200310_rgb_0020030000_ovr.jpg
Pair C, *left*, po_200310_rgb_0030020100_ovr.jpg, *right*, po_200310_rgb_0020030100_ovr.jpg

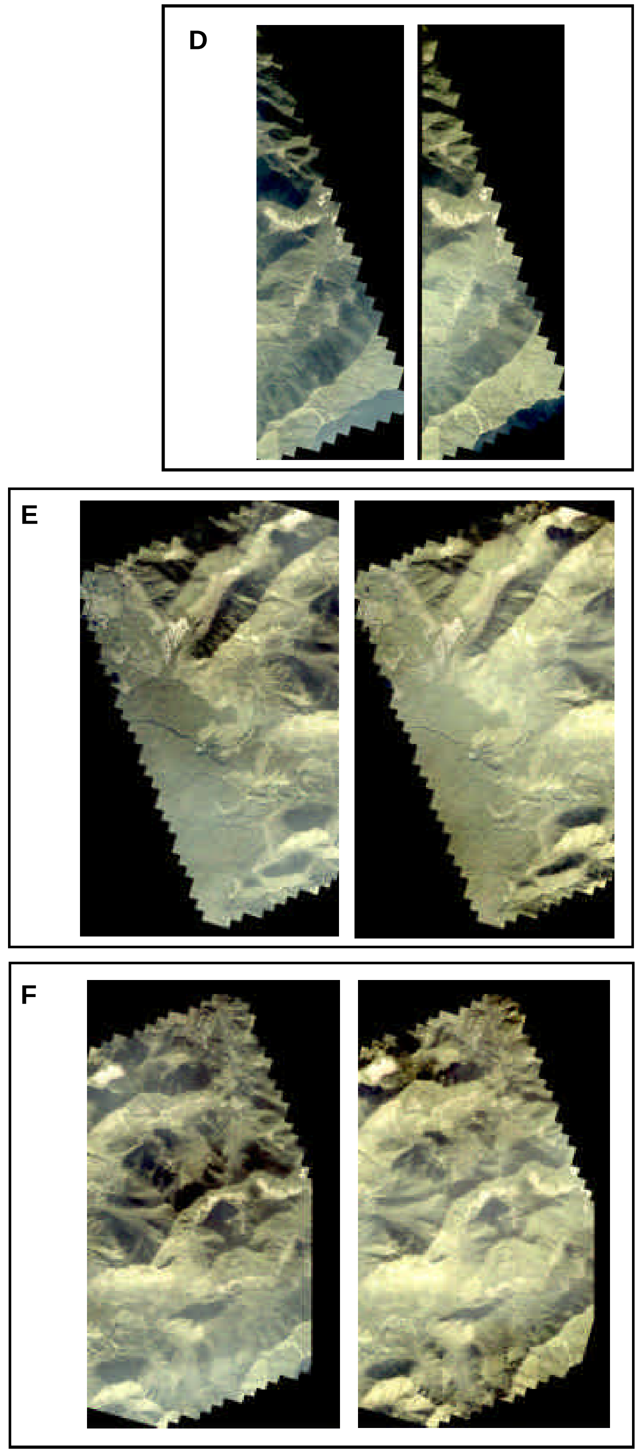

Figure 3. October 2006 IKONOS natural colour image coverage of Hesquiat / Mooyah area (stereo image pairs).

Image IDs: © GeoEye
Pair D, *left*, po_205758_rgb_0010000000_ovr.jpg, *right*, po_205758_rgb_0000010000_ovr.jpg.
Pair E, *left*, po_205758_rgb_0030020000_ovr.jpg, *right*, po_205758_rgb_0020030000_ovr.jpg.
Pair F, *left*, po_205758_rgb_0030020100_ovr.jpg *right*, po_205758_rgb_0020030100_ovr.jpg.

of the images were imaged off nadir, the ground sample distance (also known as pixel size) varied between 0.84m and 1.0m, and was resampled to a consistent 1.0m pixel size upon delivery by GeoEye. Reference stereo IKONOS imagery has a published positional accuracy of:

- 25m horizontal accuracy, and
- 22m vertical accuracy

at a 90% confidence level (CL).

There was a distinct fog or haze and more shadowing evident, due to a lower sun angle, in the October images (Figure 3) when compared with the August images (Figure 2). Metadata about each stereo pair is provided in Appendix A.

Table 2. Reference Stereo IKONOS order details.

Product Order ID	200310	205758
Date of acquisition	16 August 2006	10 October 2006

2.4 DIGITAL IMAGE PROCESSING METHODOLOGY

Image processing on this project consisted of the following major steps:

1. Creation of colour composite images;
2. Preparation of image pairs for stereo viewing;
3. Analysis of images for forest cover and landscape.

The details of each of these major steps are described in the following sections.

2.4.1 COLOUR COMPOSITE IMAGES

The following colour composite image combinations were produced from the stereo IKONOS images using ER Mapper:

a) red, green and blue channels fused with panchromatic image;

b) near-infrared, red, green channels fused with panchromatic image;

c) Guided Principal components image derived from the blue, green, red and near-infrared fused channels. As the panchromatic channel values are the same for all fused images, the panchromatic values do not add unique information for any image channel, and should not affect the individual PC factor loadings.

Image combinations a) and b) were enhanced using manual contrast stretching. Figures 4 and 5 show the three different image combinations for the central area of interest for both dates of imagery respectively. These three composite stereo pair images were loaded into a softcopy photogrammetric workstation for stereo visual analysis using polarized goggles (Figure 6).

The satellite images were also orthorectified and the same image enhancements applied for production of hardcopy plots and for presentation purposes.

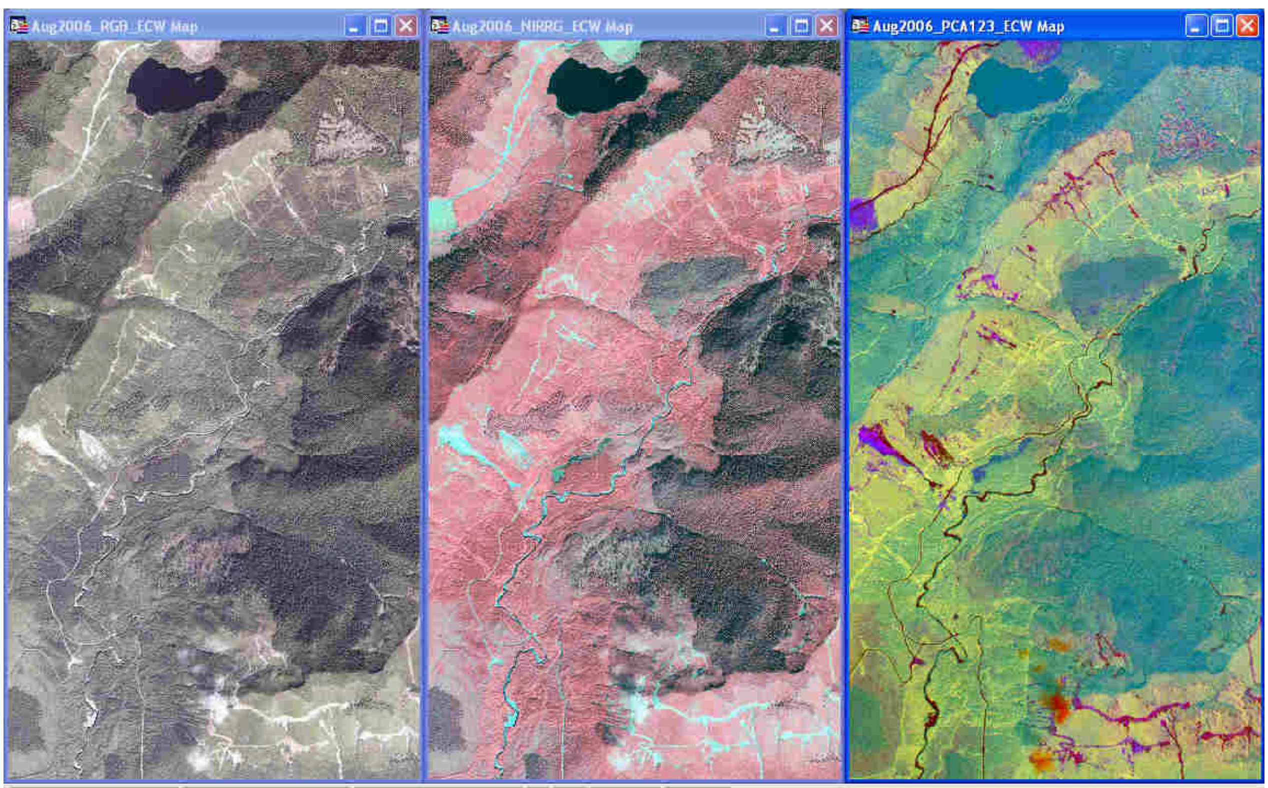

Figure 4. Different colour composite images for August 2006 imagery (Red/Green/Blue left image; Near IR/Red/Green centre image; PCA 1/2/3 right image) © GeoEye.

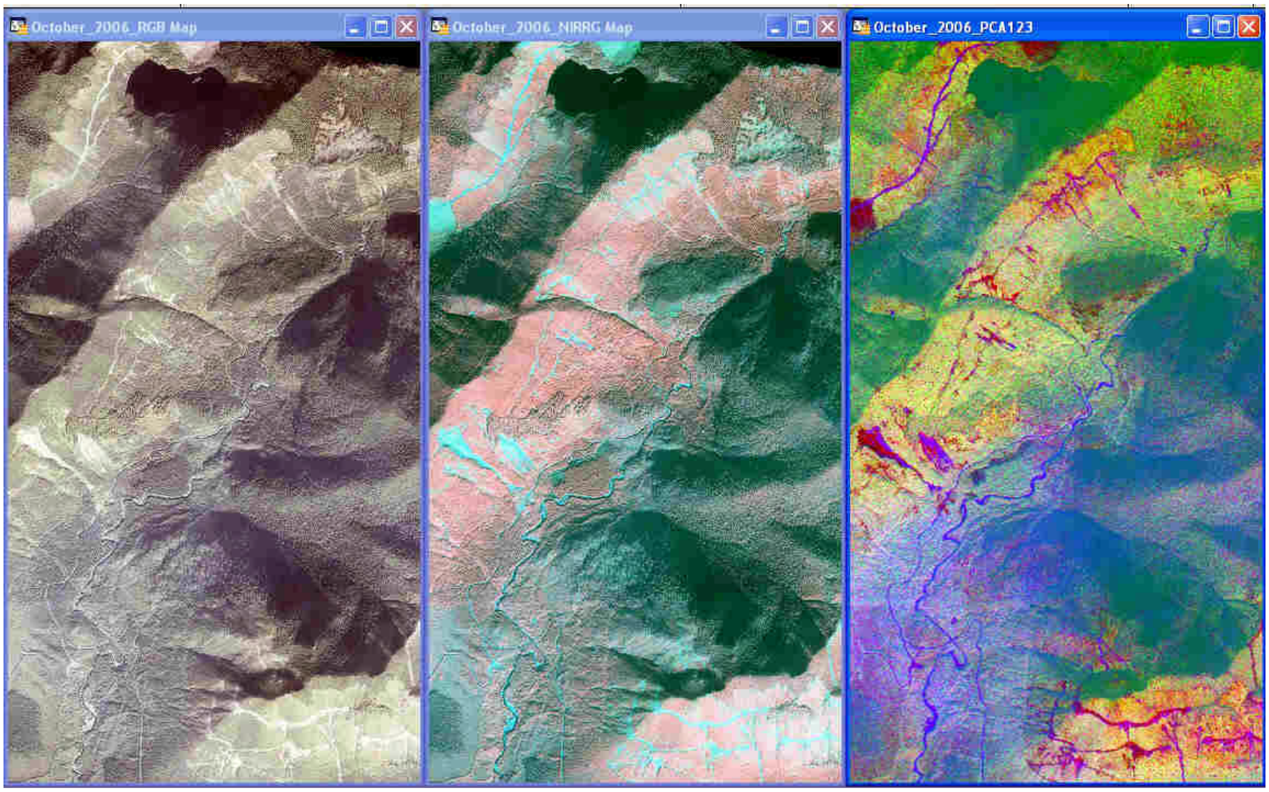

Figure 5. Different colour composite images for October 2006 imagery (Red/Green/Blue left image; Near IR/Red/Green centre image; PCA 1/2/3 right image). © GeoEye.

2.4.2 PRINCIPAL COMPONENT ANALYSIS

One of the digital processing techniques used for this project, and previous described projects (e.g., Collins et al., 2000) was Guided Principal Component Analysis (PCA), which is a form of data merging and data compression. PCA reduces the dimensionality or number of bands that the interpreter has to analyze to produce results. PCA is a statistical technique for compressing the spectral variance in multiple image bands into a subset of principal component (PC) bands, where each of the PC bands is uncorrelated with the others. This means that each PC band provides unique information not contained in the other PC bands.

The first principal components will maximize the variance across all bands in the scene as a weighted average of all the bands. The second component weights most heavily the near-infrared radiation and red bands and is an indicator of photosynthetic activity. The third and fourth components contain the remaining variance of the scene which often contains noise.

The maximum separability of no one-feature type is accomplished with PCA, although in general features can become more separable. With guided PCA, a statistical sample area is used to transform the image channels that are defined by the image analyst. In this case, we digitized polygons surrounding areas of combined forest and clearcut. The statistics generated from these polygons should maximize the spectral variation between forest and clearcut features, and allow us to potentially create a more detailed analysis of the forest area and clearcut areas. The same polygons were used for both dates of imagery (Table 3).

Figure 6. Stereo viewing of the IKONOS imagery using polarized goggles.

We chose to display PCA channels 1, 2, and 3 as Red, Green and Blue respectively. PCA 1 would have the most statistically unique information, followed by PCA 2 and 3. PCA 4 would

have the most noise. In order to aid our stereo analysis, we decided to display as much visual information as possible, and minimize noise.

The factor loadings are nearly identical for both dates, for PCA channels 1, 2, and 3. PCA channel 4 has the most difference between dates. It is possible that the haze in the October image caused the inverse in-loadings for this channel.

The following figures (Figure 7 to 9) show the individual PCA channels as greyscale images and as colour composite images for a portion of the study area.

As is typical for multispectral imagery containing both visible and near infrared channels, PC1 is mostly an average of the three visible image channels with a lesser amount contributed by the near-infrared channel. PC2 is primarily the near-infrared channel, with some difference with the red and blue channels. PC2 appears to show vegetation in bright tones (due to the high near-IR values) and soil/bare rock in dark tones. Both dates of imagery have the same rendition for PC1 and PC2, although there is a bit more shadow visible in the October imagery. PC3 is primarily a difference between blue and red light for both dates of imagery. PC3 tended to make bare soil surfaces very bright, most noticeably along forestry roads and landslides without any vegetation cover (Figure 7).

PC3 is primarily the difference between the blue and green channels, with green being negatively weighted and blue being positively weighted. PC3 has similar tones to PC2, except that the areas of lighter tones are more concentrated and road networks are more evident. PC4 has an inverse relationship between blue/green as negative loadings, and red as a positive loading. The image in Figure 8 has generally a middle greytone. There is less variability evident compared with the other PC image channels. Areas such as the northeast corner show very little difference in tone compared with the other channels. The most difference is seen in some of the bare soil/clearcut areas. We did not select this channel for the colour composite in part due to the low contrast of this channel, and also because we did not want to drop PC1 as it shows the most detail in the scene, or PC2 as it has the ratio between the near-infrared and visible light channels.

Table 3. Single date statistics for August 2006 and October 2006 IKONOS imagery.

August 2006:

Correlation Eigenvectors	PC1	PC2	PC3	PC4
Band1-blue	0.534366	-0.282411	0.752218	-0.262421
Band2-green	0.549008	-0.116753	-0.149890	0.813936
Band3-red	0.543245	-0.193545	-0.637021	-0.511497
Band4-NIR	0.343406	0.932284	0.076846	-0.083750

October 2006:

Correlation Eigenvectors	PC1	PC2	PC3	PC4
Band1-blue	0.521186	-0.321406	0.766705	0.192945
Band2-green	0.534149	-0.154281	-0.226520	-0.799732
Band3-red	0.529900	-0.218821	-0.593971	0.564378
Band4-NIR	0.402811	0.908302	0.089730	0.068399

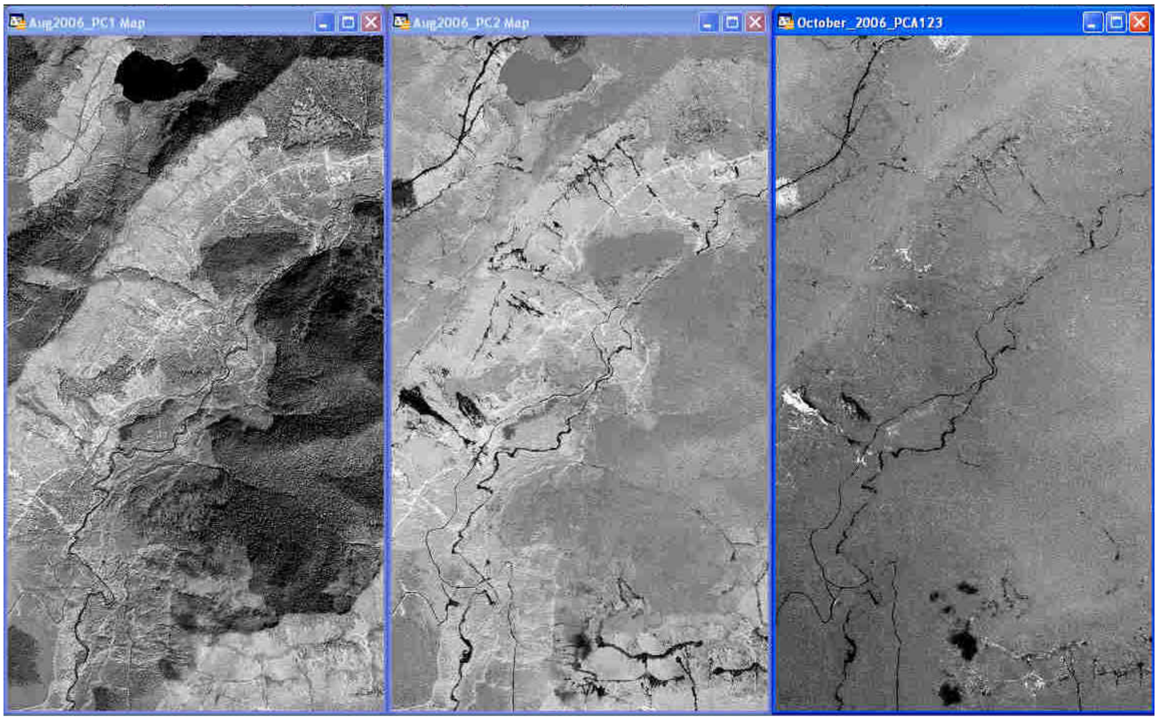

Figure 7. PCA channels 1, 2 and 3 from August 2006 image. © GeoEye

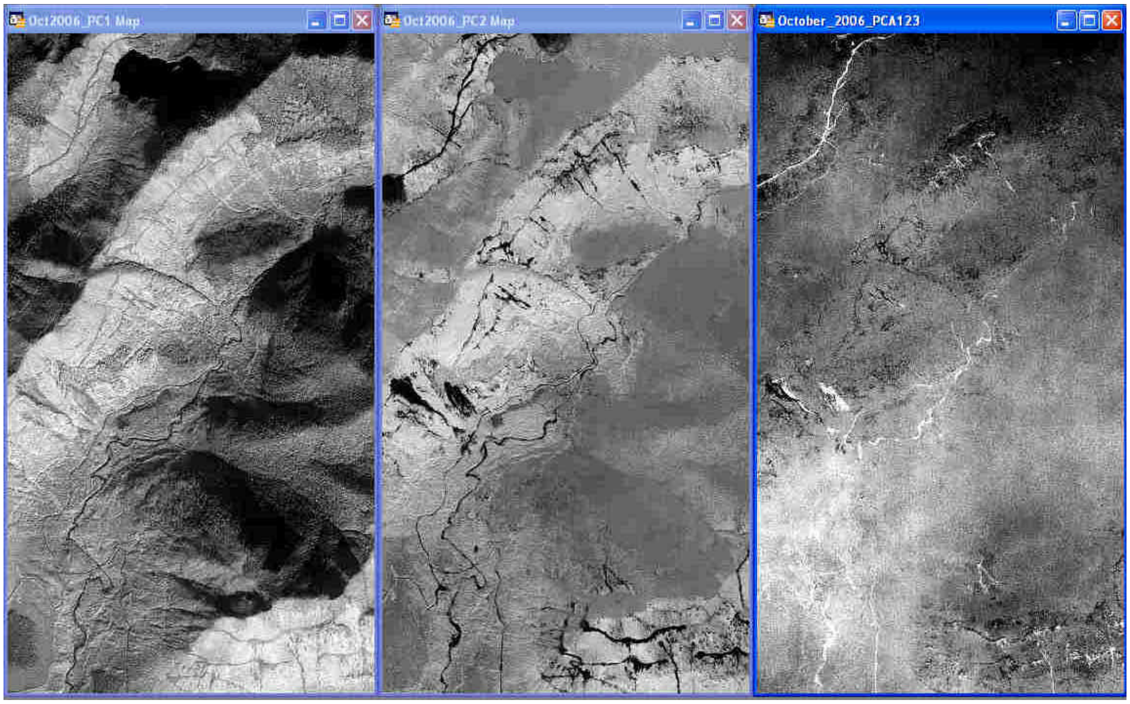

Figure 8. PCA channels 1, 2 and 3 from October 2006 image. © GeoEye

In Figure 9, newly cleared forest areas, roads, and slide areas show up with reddish or purple tones. Revegetated areas (typically with alder) appear in yellow tones and forested areas are in green-red tones. Water bodies appear in dark hues. The October image appears to have more contrast, which is likely a combination of shadows caused by lower sun angle and fog or haze.

2.5 PHOTOGRAMMETRIC ANALYSIS

2.5.1 DATA IMPORT

The KLT softcopy photogrammetric software was used for stereo setup and viewing (www.kltassoc.com). To get the IKONOS stereo pairs into the KLT, we needed to take the individual image channels, blue, green, red, and near-infrared, and generate the RGB, NIR and Principal Component colour composites. The KLT software works with 24 bit colour TIF images (8 bits for each of the red, green, and blue channels that make up a colour image). As the IKONOS imagery has 11 bits per channel, we needed to compress the individual channels into 8 bits in order to produce the 24 bit colour composite TIF images.

The TIF images were also enhanced for stereo viewing and overview pyramids were created for quick zooming. In this particular example, there were two stereo pairs with approximately the same stereo coverage.

Set 1 is from August 2006 and uses the following files:

- Left image 200310_RGB_0030020000.tif, and
- Right Image 200310_RGB_0020030000.tif.

Set 2 is from October 2006 and uses the following files:

- Left Image file po_205758_RGB_0030020000.tif, and
- Right image file po_205758_RGB_0020030000.tif.

2.5.2 SATELLITE IMAGE AEROTRIANGULATION

After importing the images, the next step is to set up the "model" space for the imagery to be viewed in real world coordinates. To do this, the KLT read the corresponding Rational Polynomial Coefficients (RPC) text files for each of the left and right images and created a stereo model setup. The stereo IKONOS imagery is supplied with RPC files, which contain a series of coefficients used to describe the relationship between the image as it existed when captured and the Earth's surface. The RPC files contain information that is needed to determine "interior" and "exterior" orientation, as well as supplemental information such as the geographic coordinates associated with the coordinates of the imagery. The exterior orientation of a camera defines its location in space and its direction of view. The "interior" orientation defines the geometric parameters of the imaging device, which is primarily the focal length of the lens, but can also include a description of lens distortions.

Two stereo model setups were created: one for August and one for October (Figure 10). An identical location was observed for both stereo pairs at:

- August UTM Zone 9 coordinates 681810.6mE, 5491481.9mN, 98.9m
- October UTM Zone 9 coordinates 681812.1mE, 5491477.1mN, 89.3m

The discrepancy in metres between the two models is X=2, Y=5, Z=10. According to GeoEye the elevation from the RPC files are Ellipsoidal.

The next step was to try to improve the absolute positional accuracy, based on ground control points obtained with a handheld GPS during ground truthing. There were no targets on the ground

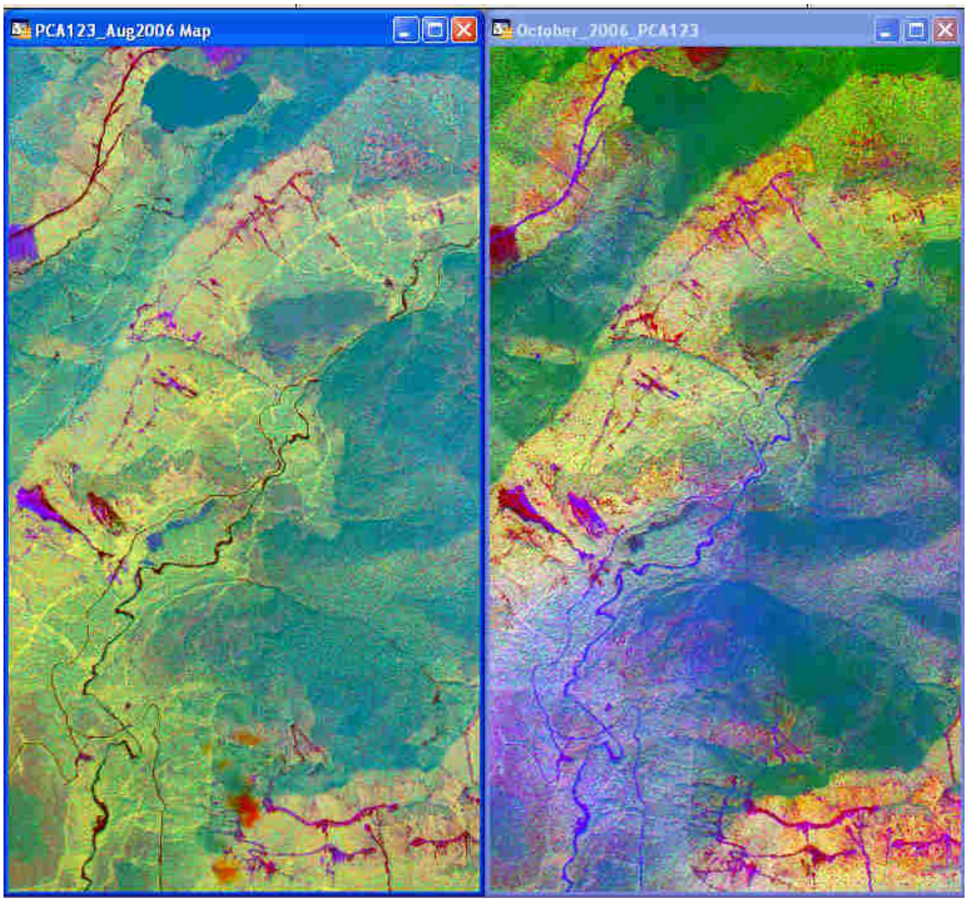

Figure 9. PCA colour composite images for the IKONOS imagery. August image is at left, October image at right. © GeoEye

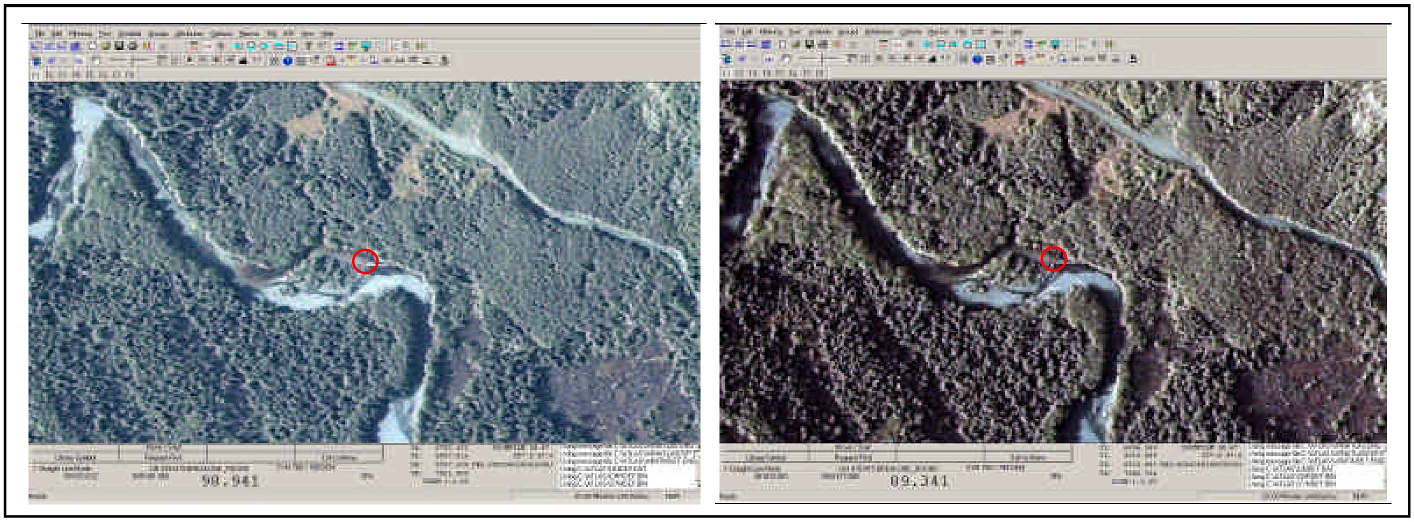

Figure 10. August image coordinate (shown as a red dot surrounded by a red circle) at left, and October image coordinate at right for aerotriangulation. © GeoEye

(i.e., for aerial photography, highly accurate GPS coordinates are acquired for an area and "targets", usually a white coloured x or cross, are placed at each location; these locations are captured during the aerial image acquisition) at the time of satellite image acquisition, so the positions are only estimates. In addition, the handheld GPS is only accurate to between 5-10m. We also assumed the handheld GPS vertical elevations are Geoidal. We used 13 GPS control points spread across the image to help more accurately position the satellite imagery (Table 4).

Table 4. The control point locations.

ID	Easting (m)	Northing (m)	Elevation (m)
19	684660.69	5488198.85	261
20	684695.52	5488131.15	251
21	679148.16	5491380.69	258
1	681430.29	5485352.57	292
10	678107.67	5490559.13	31
13	682224.01	5495084.27	707
14	685110.13	5496381.47	340
15	685475.66	5491917.60	589
2	683815.57	5486466.40	570
3	680903.97	5487208.94	146
5	685956.95	5489330.10	170
7	683356.41	5489619.41	483
8	683518.27	5489938.13	687

Using the KLT, approximate locations for each control point were observed monoscopically on all four frames simultaneously, and marked (Figure 11).

After all the control points were input, a bundle adjustment was run on all four frames and two stereo models. The role of a bundle adjustment is to minimize the sum of the squares of a set of errors between the observed and predicted image points in an image, by using a non-linear, iterative set of real-valued functions. The results of the bundle adjustment are based on one "base" frame, which has the other three frames as reference to it. In this case, frame "August Left 200310_RGB_0030020000.tif" was used as the base frame. The results of the bundle adjustment are detailed in Appendix B.

After the bundle adjustment, the same check location (Figure 12) was observed to have the following UTM Zone 9 coordinates:

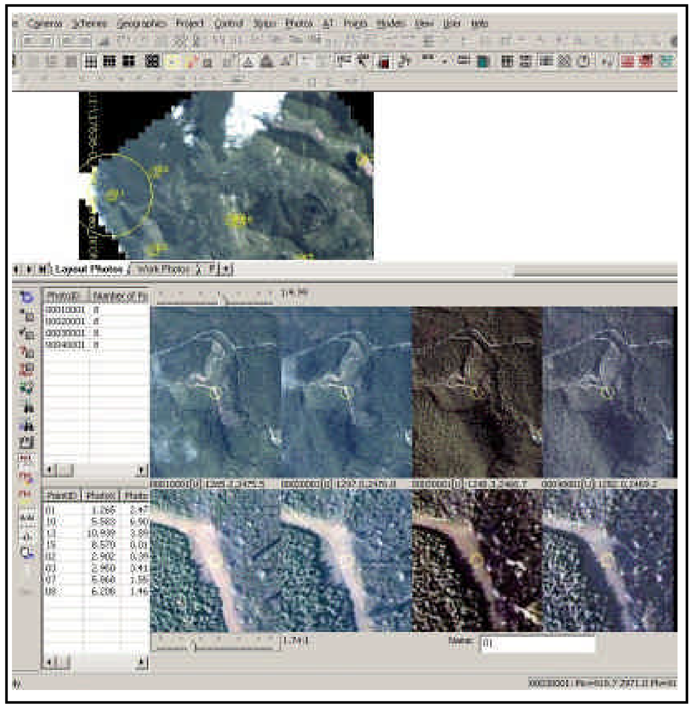

Figure 11. Viewing the control point locations monoscopically in the KLT. © GeoEye

- August 2006: 681809.4mE, 5491491.1mN, 110.0m
- October 2006: 681812.3mE, 5491487.7mN, 105.2m

The discrepancy in metres between the two models is now X=3, Y= 3, Z=5

The elevation after the GCPs were read was 10 and 20 metres higher respectively than the original Ikonos RPC setups. The elevation difference could be due to the difference in elevation between the earth as an ellipsoid and earth as a geoid at this location on the earth. There may also be positional differenced

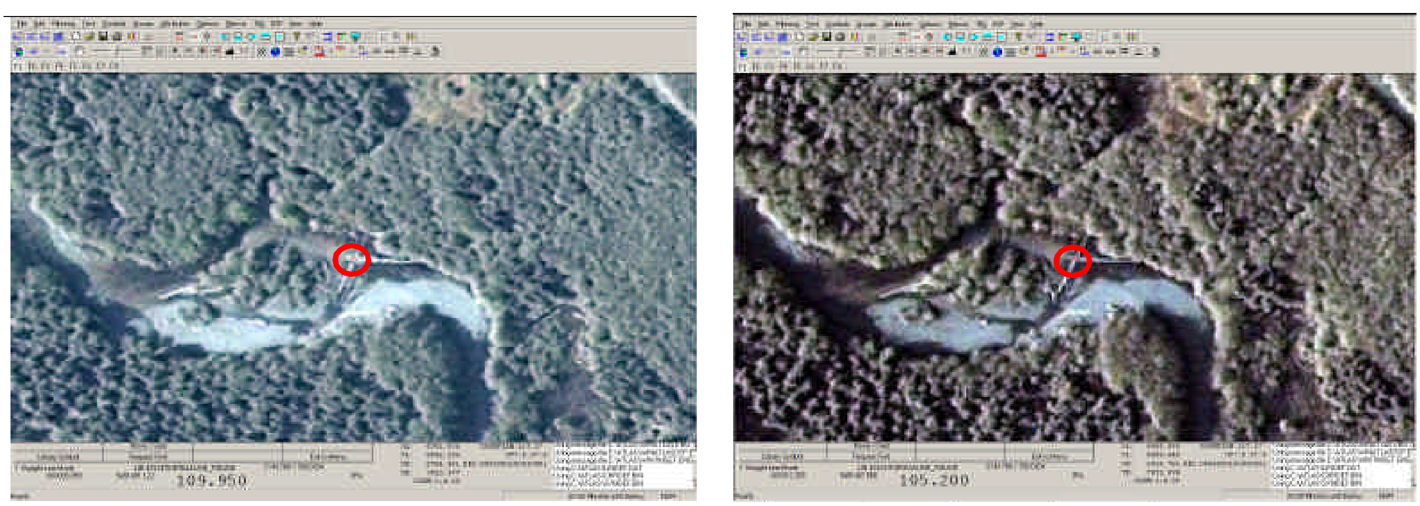

Figure 12. August image coordinate (shown as a red dot inside the red circle) at left and October image coordinate at right for after bundle adjustment. © GeoEye

between the two dates inherent in the RPC files.

2.5.3 PHOTOGRAMMETRIC COMPILATION

For this project, we attempted to photogrammetrically compile the following types of features:

- spot heights and break lines (for the generation of a Digital Elevation Model [DEM]);
- landslide features;
- forest cover stands.

2.5.3.1 DIGITAL ELEVATION MODEL

For the DEM, the photogrammetrist worked with the August 2006 image. The operator used the natural colour RGB image for the compilation. A valley within the northeast portion of the stereo pair was selected for data collection and DEM creation. The compilation for this 9 sq km region took approximately seven hours (one working day). Both IKONOS satellite imagery and scanned TRIM aerial photos have a spatial resolution of 1m. After generating the DEM using IKONOS, we compared our results to a TRIM-derived DEM for the same area. Spot heights were sampled approximately every 40 m in the IKONOS image. The area of interest is shown in Figure 13.

The spot heights and break lines were saved as 3D AutoCAD files. The break lines were saved as points, then both point files were imported into MapInfo Professional format. A TIN model function was used to convert the points into a DEM with 10x10m grid cells (Figure 14). The TRIM DEM for the same area was also imported into MapInfo Professional, then the two DEMs were subtracted to produce a difference grid (Figure 15). Statistics were calculated on the minimum, maximum, mean, variance, and standard deviation values for the grid difference values (Table 5).

Table 5. DEM statistics calculated for IKONOS, TRIM, and the differenced grid.

DEM statistics for IKONOS:	
Minimum	140
Maximum	1060
Mean	494.064297
Variance	34156.096777
Standard Deviation	184.813681
DEM statistics for TRIM:	
Minimum	140
Maximum	1080
Mean	496.436125
Variance	36414.180213
Standard Deviation	190.824999
DEM statistics for the differenced grid:	
Minimum	-86.281982
Maximum	81.959442
Mean	7.315228
Variance	124.650540
Standard Deviation	11.164701

There are some edge effects in the IKONOS DEM as the points collected did not extend beyond the limit of the gridded region. This is very noticeable in the SW corner of the IKONOS DEM. The comparison between the two DEMs and contours was done away from the edges of region of interest, in order

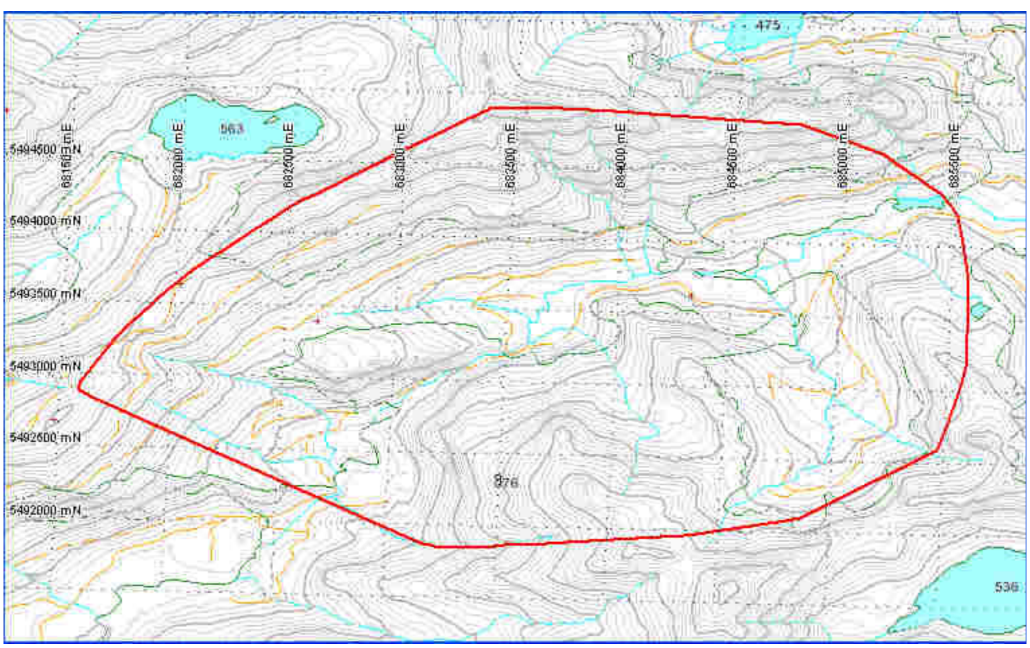

Figure 13. Location map of area chosen for spot height and break line collection (UTM Zone 9, NAD83).

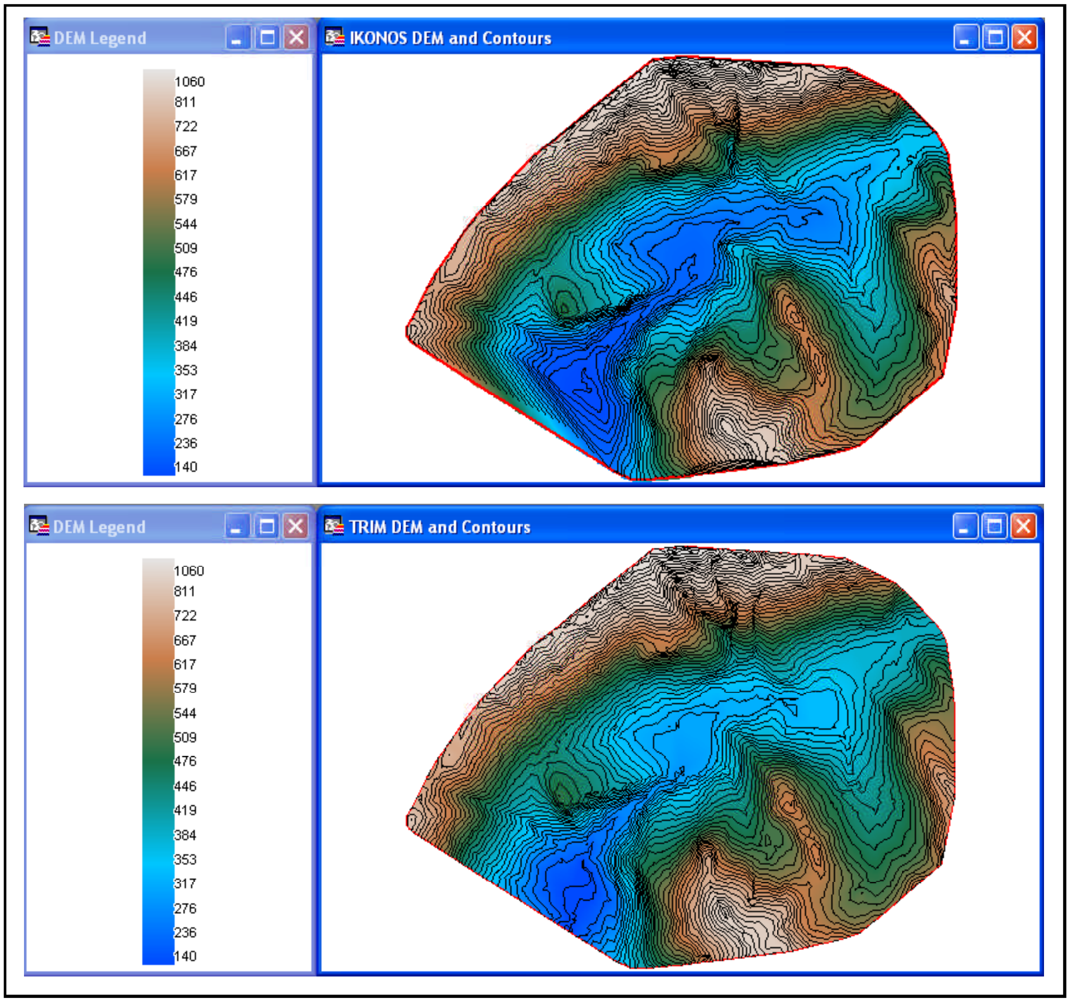

Figure 14. Stereo IKONOS derived contours (top) and corresponding TRIM contours (bottom).

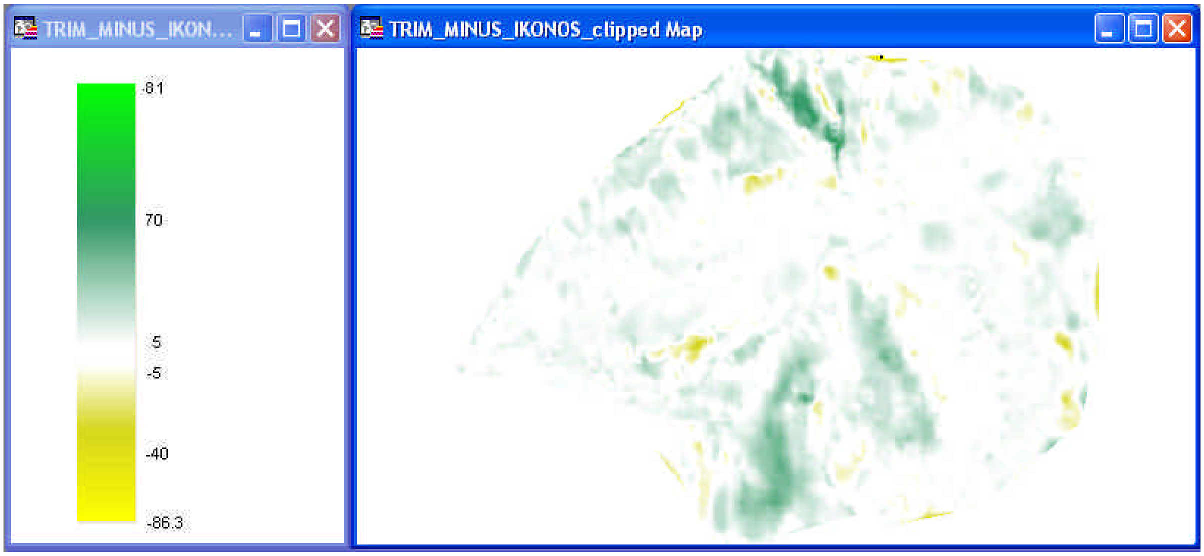

Figure 15. Differenced grid between IKONOS and TRIM DEMs. Difference values in metres.

to remove artifacts caused by lack of data at the edges.

The largest positive and negative values occur at the edges where there are edge effects due to data collection and gridding of the IKONOS spot heights. Visually, a large portion of the data appear to fall within the -5 to +5 m range. Large positive values indicate the IKONOS DEM values are lower than the TRIM DEM values, while large negative values indicate larger IKONOS DEM values than the TRIM DEM values. For this area of interest, it appears that the TRIM DEM values are more often larger than the IKONOS DEM values.

2.5.3.2 LANDSLIDE FEATURES

The elevation points and break lines covering the largest landslide in this scene was photogrammetrically compiled using the October 2006 image. We used the natural colour RGB image for the compilation.

The spot heights and break lines were sampled between 4-9m within the slide area and 15m around the slide area margins. The spot heights and break lines were saved as 3D AutoCAD files. The break lines were saved as points, then both point files were imported into MapInfo Professional format. A TIN model algorithm was used to convert the points into a DEM with 3x3m grid cells. The spot heights and break line points and image are shown in Figure 16.

A determination of the volume of material that has been removed by the landslide is of interest. As we did not have a pre-landslide stereo pair image, we created a pre-landslide DEM by removing the spot heights and break line points from the interior of the landslide, and regridded, based on the sample points at the edges of the slide. We used TIN gridding which generated flat facets across the slide area. We did not want to make any assumptions as to the convexity of the across-slope curvature, so did not use a gridding algorithm to add convexity. Figures 17 and 18 show the theoretical pre-slide grid, the post-slide grid, and the differenced grid.

From the differenced grid we summed up the differenced values to determine the volume of material removed by the landslide. The value calculated through this approach is 368,419.29 cubic metres. If the pre-slide area had a drainage channel then the actual volume would be less than our calculated volume.

We also generated a slope magnitude digital landform model (DLM) from the post-slide grid, which is shown in Figure 19. Descriptive statistics for the slope magnitude DLM were also produced (Table 6).

2.5.3.3 FOREST COVER

For the forest cover interpretation, all three colour composite images were viewed in 3D and monoscopically. In addition, both the August and October images were viewed. With the satellite orbital elevation of 681 km, the viewing angle although off-nadir for stereo viewing, still provides the operator with near-vertical views of the tree canopy. This proves useful in dense forest stands as the operator can see between the trees in many cases.

The Ministry Inventory Forester we worked with was most comfortable viewing the natural colour RGB image in 3D. There was also a preference for the August image due to the more

Table 6. Landslide statistics.

Descriptive statistics for differenced grid:	
Minimum	0.200226
Maximum	32.493896
Mean	9.121095
Variance	61.974133
Standard Deviation	7.872365
Descriptive statistics for slope magnitude grid:	
Minimum	0.777220
Maximum	94.064407
Mean	26.555110
Variance	246.545981
Standard Deviation	15.701783

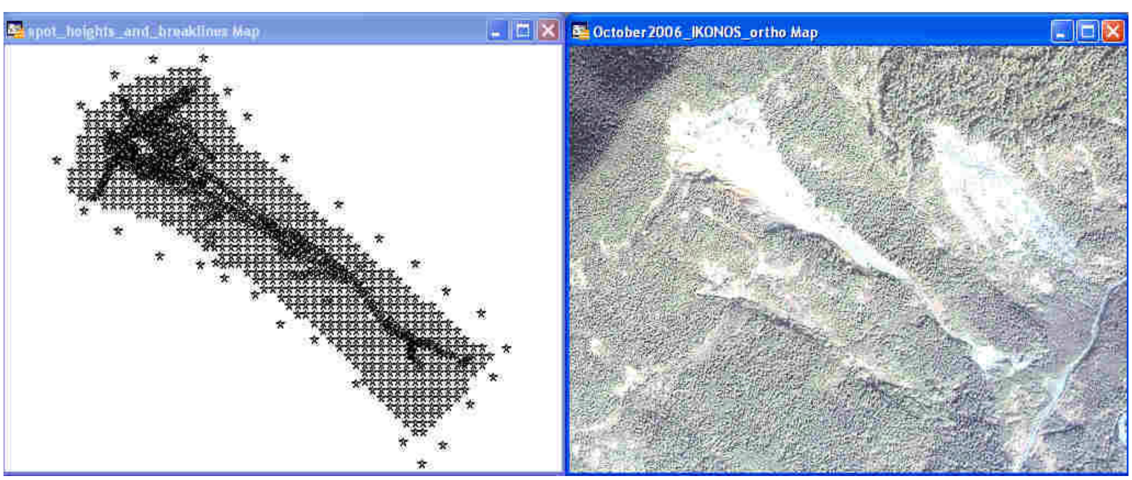

Figure 16. Spot heights and break line points on the left and image on the right. © GeoEye

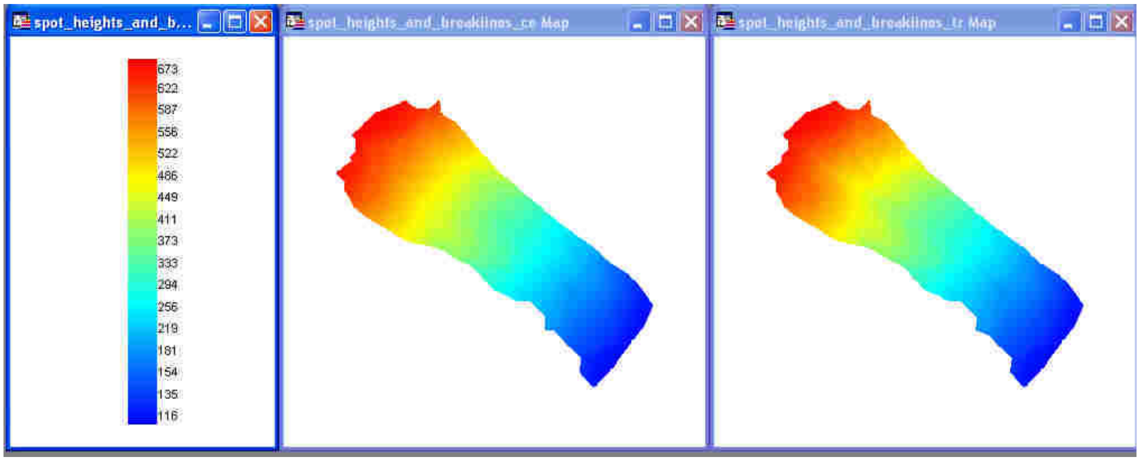

Figure 17. Pre-slide grid on the middle and post-slide grid on the right. Elevation legend on the left. Values are in metres.

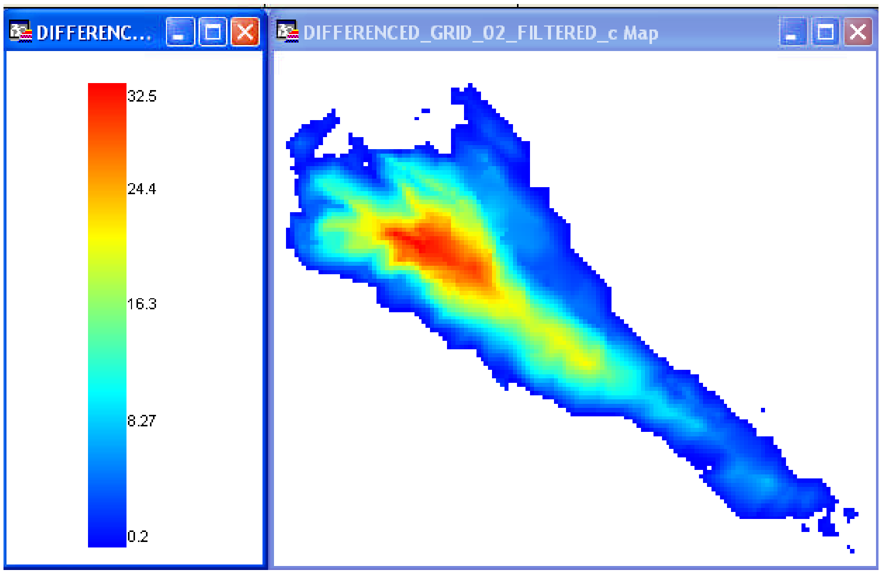

Figure 18. Differenced grid. Largest difference is in the red coloured area. Values are in metres.

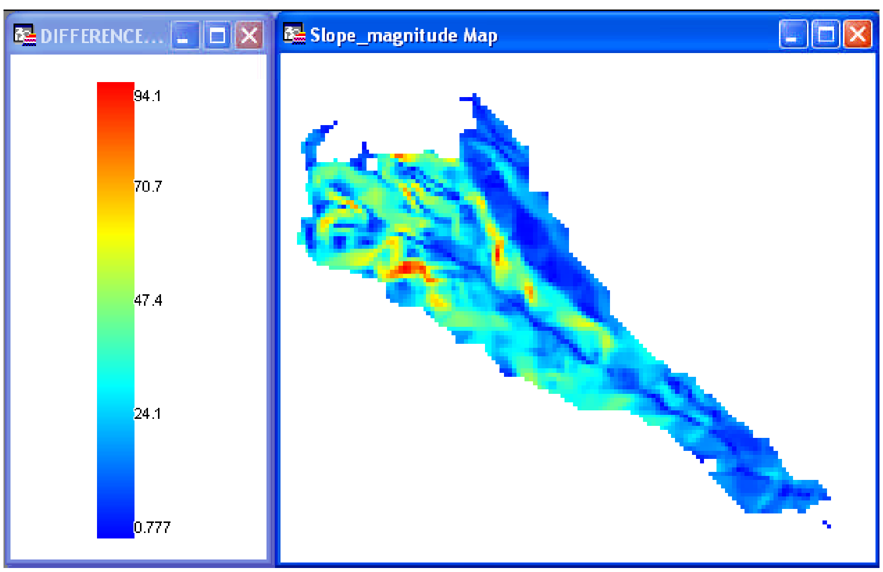

Figure 19. Slope magnitude digital landform model. Slope in degrees.

vibrant colours. The October image tended to have less saturated (tending toward greytones) colour. Through our analysis it was noted that neither the natural colour nor the false colour infrared composite on their own provided the best image for interpreting all features. It was recommended that both the natural colour and the false colour infrared composites be used for image interpretation. The Principal Component image, although not chosen for more in-depth stereo viewing, did appear to outline each tree crown, making individual trees appear more distinct from their surroundings. This could prove useful for counting trees within a forest cover stand.

Some general comments on the images by the interpreter:

- The August 2006 image shows tree species composition better than the October image, which has less colour differentiation and deeper shadowing, and is more “greyed out” overall;
- Textural changes due to differences in tree heights and species can be seen, especially when changes in terrain are also evident;
- Colour differences between various tree species are not easy to distinguish compared with hard copy air photos at a similar viewing scale. For example, the usual yellowish colour signature of cedar and cypress crowns does not show up very well;
- Distinguishing individual trees by species is not easy. Neither colour variation nor crown shapes is well-defined. There is insufficient depth in viewing the tree canopies and branching patterns;
- Some additional clues in interpreting species composition are gathered from shadows cast by tree crowns onto roads, open ground, and water bodies. These shadows give a better view of the crown shapes than are visible within the stands;
- Use of the near-infrared channel does not help with species identification. In most cases, the tree crowns are fragmented into different colours/hues, and overall shape is less evident;
- Near-infrared does highlight age differences, especially between old growth trees on poor sites and regeneration/ second growth on more productive sites. Non-vegetation features such as rock outcrops and exposed soil also stand out more;
- As with air photos, the spike tops on old growth cedars do not resolve on the image. When measuring these tree heights the “missing” tops must be accounted for;
- Generally, height measurements made on the image correlate quite well with both ocular estimates and attributes from the forest cover map, as long as the ground is visible. The more open the stand and the taller the trees, the easier it is to make accurate height measurements;
- Height measurements from the image do not correlate as well with map values where part of the original map polygon has been logged and the labels not adjusted to account for removal of the higher volume area of the stand.

Twenty three forest cover polygons were interpreted from the satellite imagery without reference to the existing forest cover map. These polygons and satellite imagery were later overlaid on existing forest cover map of the area (Figure 20). We noted that the satellite image showed more harvested blocks compared with the map, as the imagery is more recent than the forest cover maps. The forest cover map polygons have a photo interpretation date between 1990 and 1997, although there are some with dates of 1986 and 1969.

Observations on overlay of satellite interpreted polygons on existing forest cover map:

There are 23 satellite interpreted polygons (Figure 21). One of the polygons was outside of the boundaries of the forest cover map and another polygon represented a non-forest type. This leaves 21 satellite interpreted polygons for discussion (Figure 22). We overlaid our satellite interpreted polygons on top of the existing forest cover map polygons to check for similarities and differences between interpretations and polygon boundaries. Through the use of spatial overlay in MapInfo Professional we determined that each satellite-interpreted polygon generally overlaps with three forest cover map polygons. Each of the satellite-interpreted polygons tends to be almost entirely enclosed by one forest cover map polygon. The additional overlaps form slivers along the margins of the satellite-interpreted polygons.

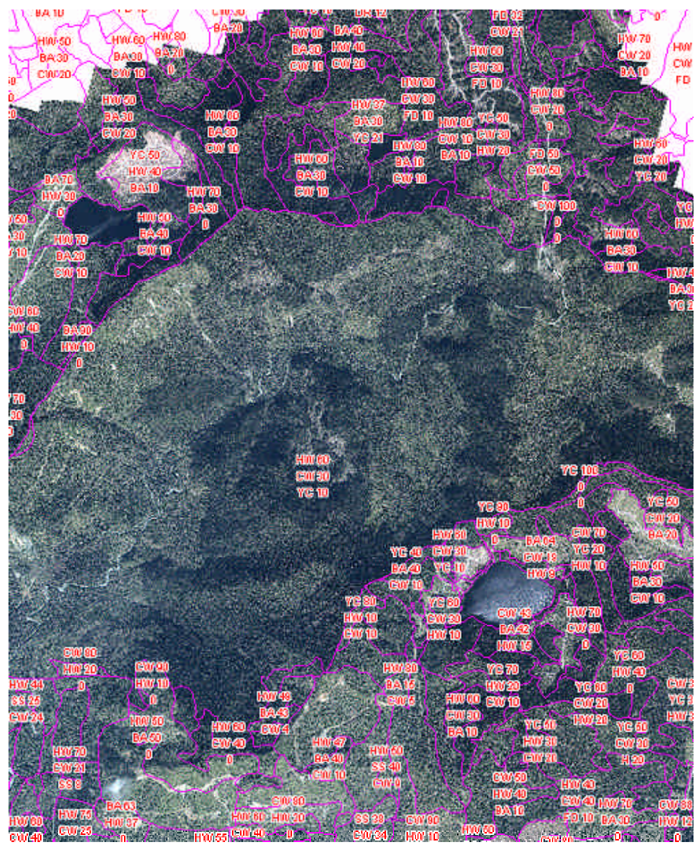

Figure 20. Existing forest cover map overlaid on August satellite imagery. The top three tree types along with their percent coverage are provided as labels. © GeoEye

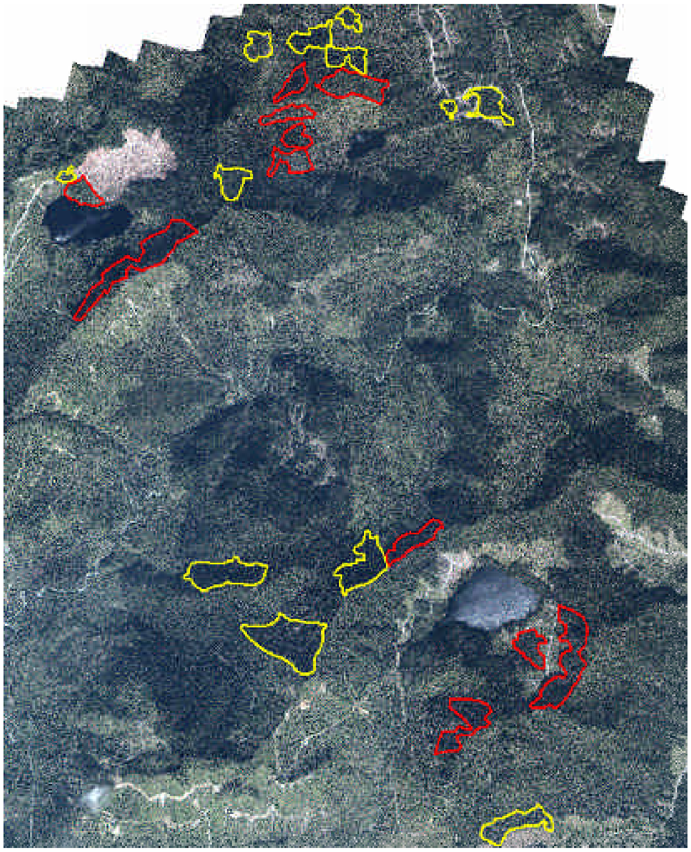

Figure 21. Interpreted forest cover polygons from the August satellite imagery. Red polygons were interpreted from the natural colour, RGB image, and the yellow polygons were interpreted from the false colour infrared imagery. Twenty-three forest cover polygons were interpreted. © GeoEye

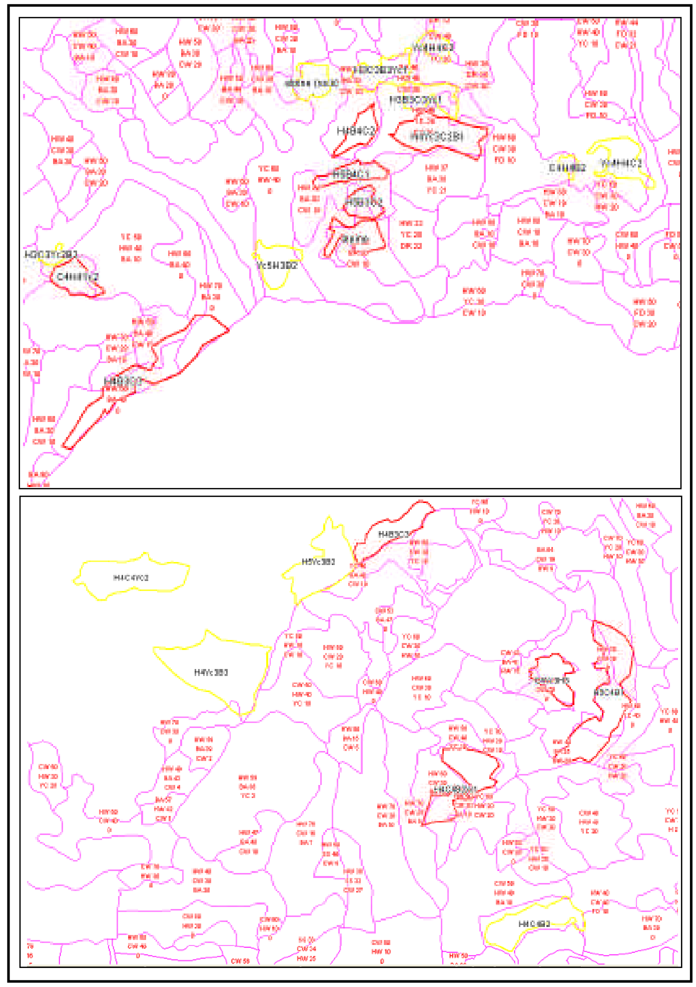

Figure 22. The satellite interpreted polygons overlaid on the existing forest cover map. North (top) and south halves are shown separately to allow for enlargement.

Figure 23. Overlay of polygon 4 (red line) on top of the forest cover map. © GeoEye

The descriptive statistics about the number of overlapping polygons between the two datasets are as follows.

Minimum overlaps:	1
Maximum overlaps:	6
Mean overlaps:	3.04762
Standard Deviation:	1.36194

The satellite-interpreted polygons cover homogeneous regions in the image, while the existing forest cover map polygons tend to show more variation in forest cover types. Figure 23 shows a typical satellite interpreted polygon overlaid on the forest cover map.

Observations of the RGB and NIR colour composite images and the satellite derived polygons:

Each of the interpreted polygons are shown in the following figures (Figures 24 to 46), overlain on both the RGB image (on the left) and the near-infrared (NIR) image (on the right). Beneath each image are brief notes by the interpreter.

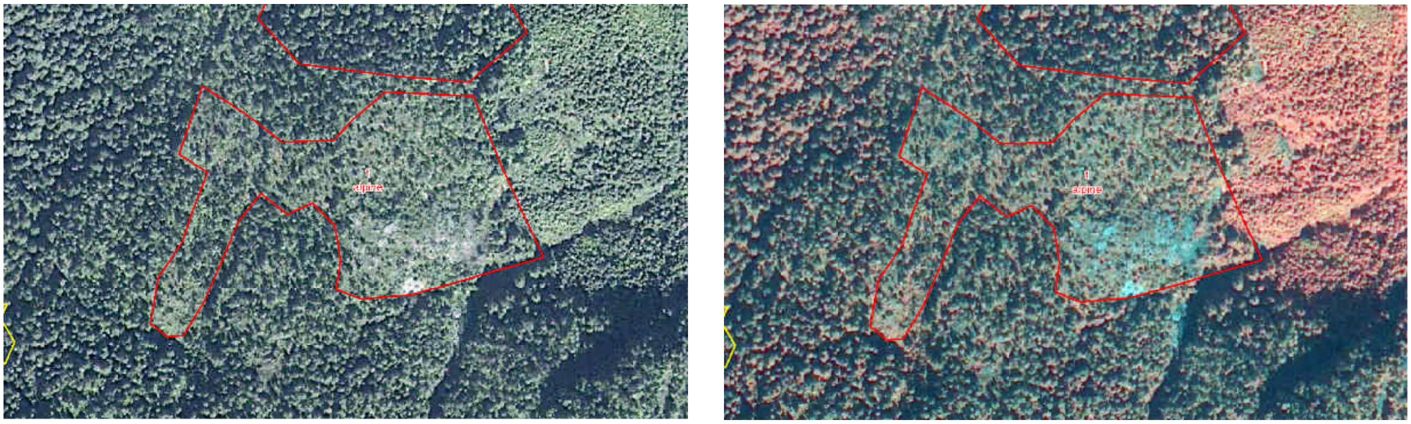

Figure 24. Polygon 1. RGB: Small scattered trees, difficult to interpret species but crown shadows help identify presence of amabilis fir. NIR: Tree species harder to identify but easier than with RGB to pick out rock outcrops. Dramatic colour shift to red in adjacent vigorous second-growth stand. Boundary between mature and young forest is sharply defined. © GeoEye

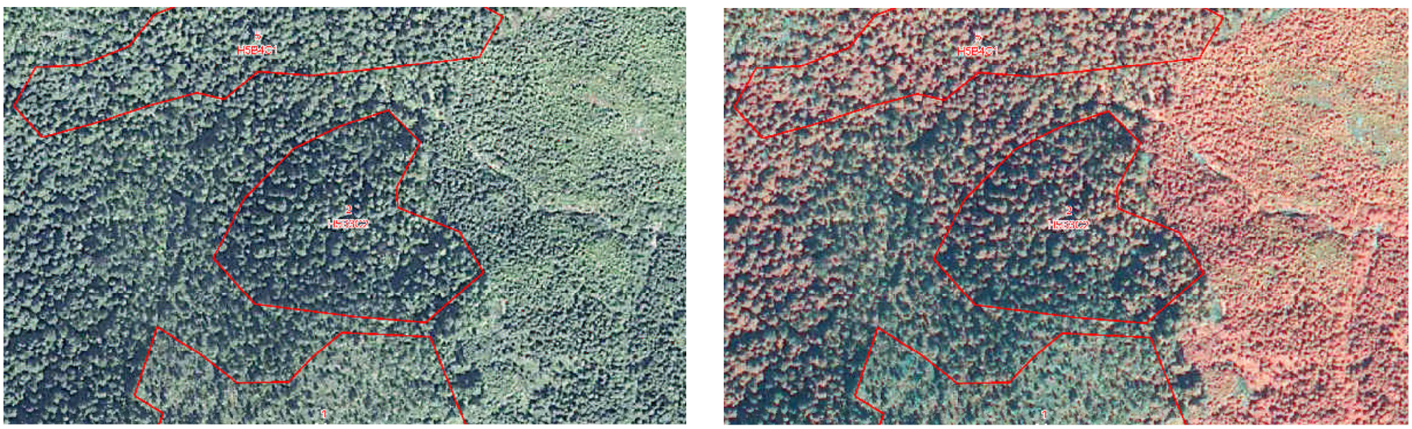

Figure 25. Polygon 2. RGB: Deep shadows within stand makes it hard to see crown shapes. NIR: Tree species harder to identify because of colour separation in the crowns. Again, note dramatic colour change in adjacent vigorous second growth. © GeoEye

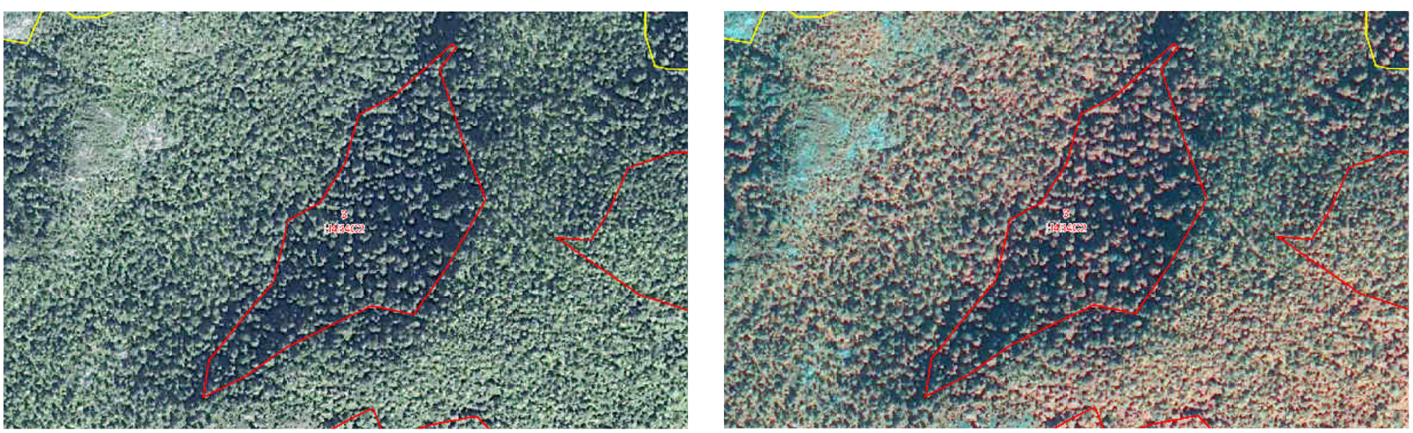

Figure 26. Polygon 3. RGB: Deep shadows within stand makes it hard to see crown shapes. NIR: Tree species harder to identify because of colour separation in the crowns. © GeoEye

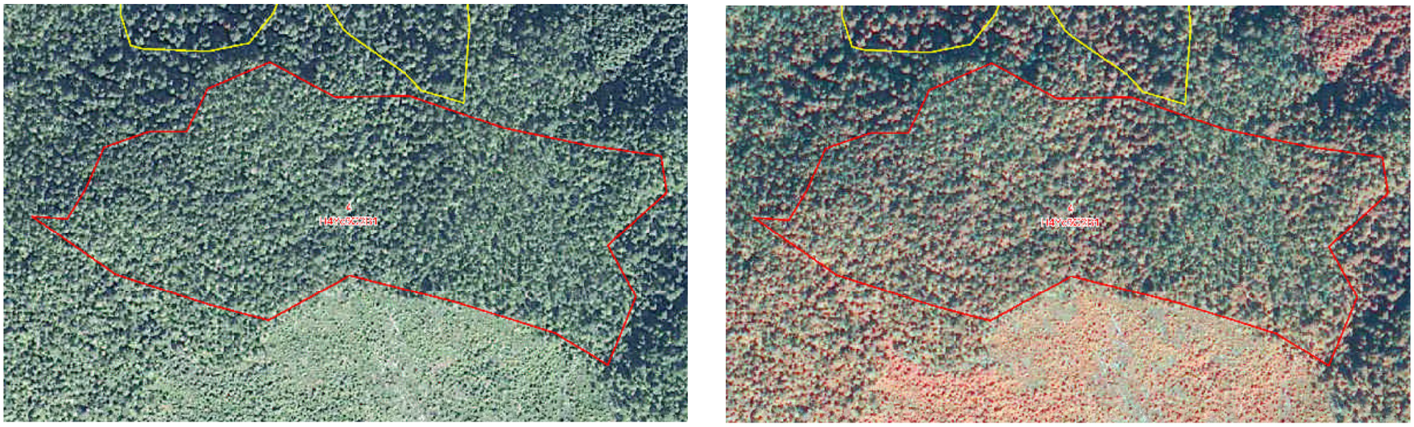

Figure 27. Polygon 4. RGB: High elevation stand with cypress. Hard to distinguish shapes of small crowns. NIR: Same comments as for polygons 2 and 3. © GeoEye

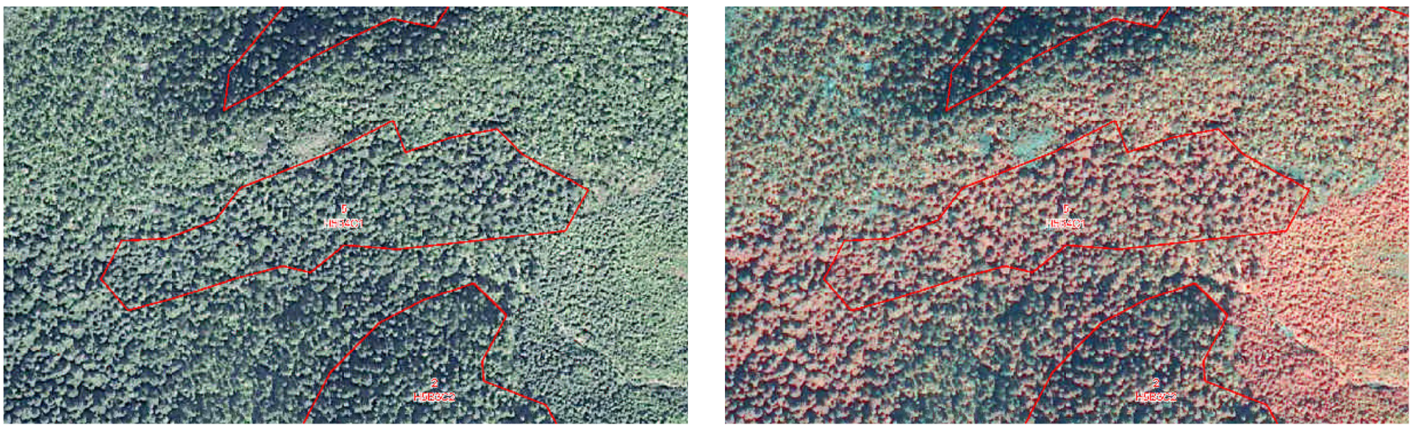

Figure 28. Polygon 5. RGB: Less shadow than polygons 2 and 3. Easier to distinguish tree crowns. NIR: Brighter aspect than polygons 3 and 4. NIR not helpful in identifying species. © GeoEye

Figure 29. Polygon 6. RGB: Low productivity stand with large component of cedar and cypress. Small trees but species ID helped by long shadows cast on roadway. NIR: No help with species ID. © GeoEye

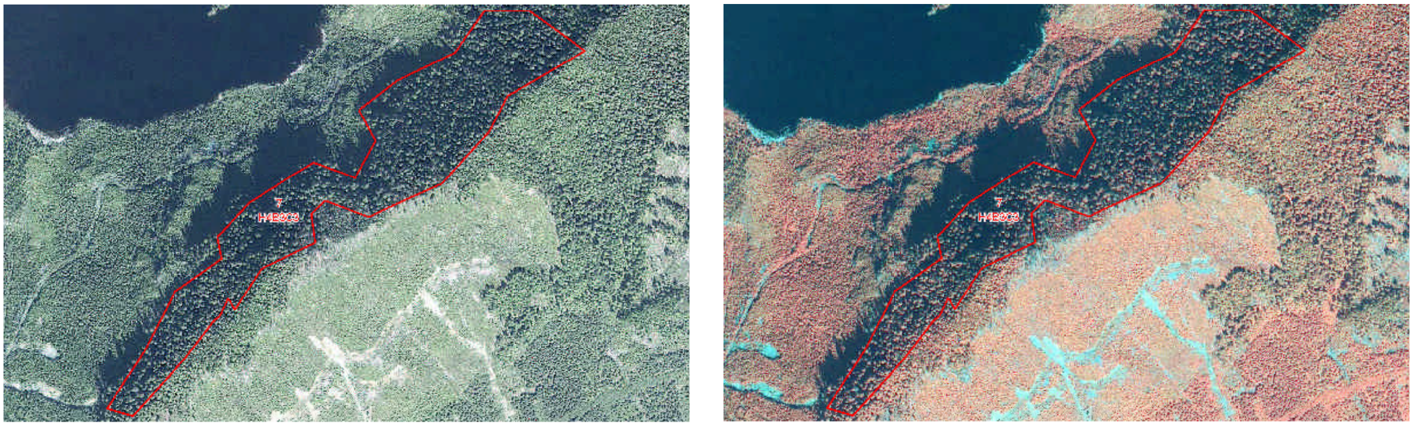

Figure 30. Polygon 7. RGB: Ridge top hemlock / balsam stand. Small crowns but note very long shadows cast at bottom of slope which assists species ID. NIR: Alder regeneration on old roads highlighted by NIR. © GeoEye

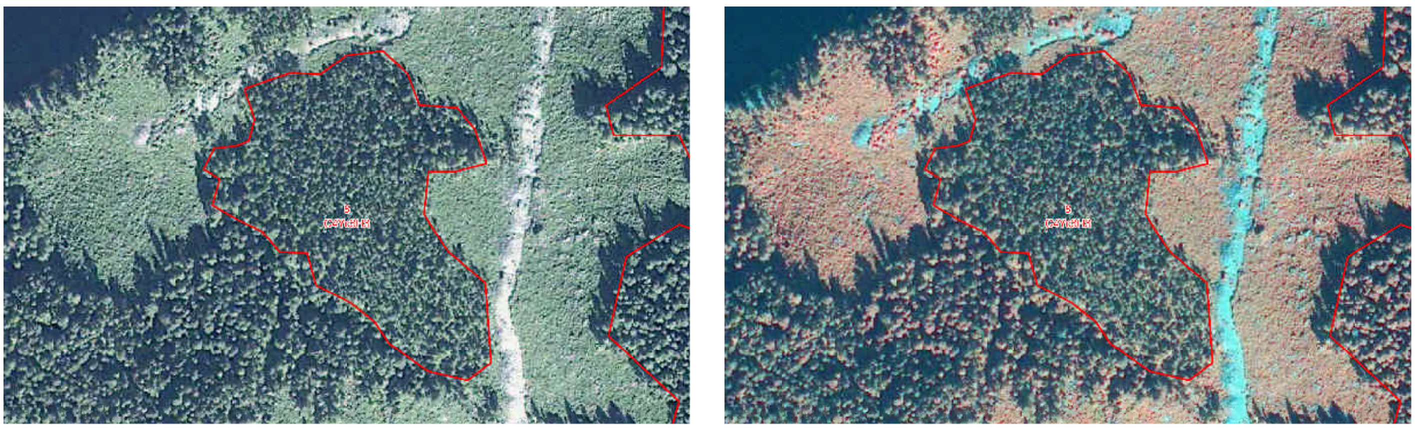

Figure 31. Polygon 8. RGB: Poor cedar/cypress site with small trees. Species ID difficult but aided by crown shadows.NIR: Same as polygon 6. © GeoEye

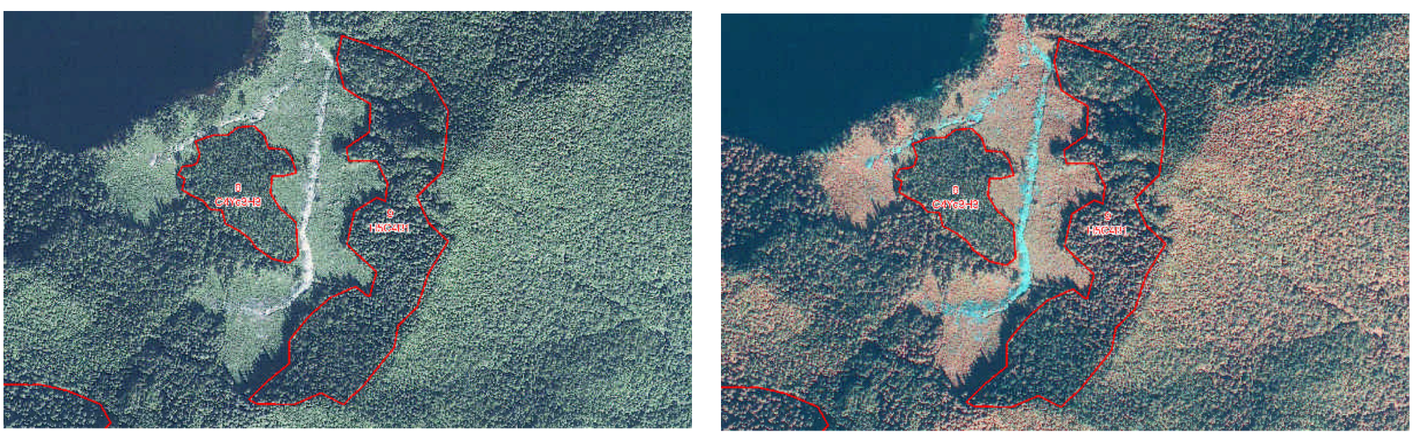

Figure 32. Polygon 9. RGB: Better site than polygon 8 with larger trees which are easier to identify. NIR: No help with species identification. © GeoEye

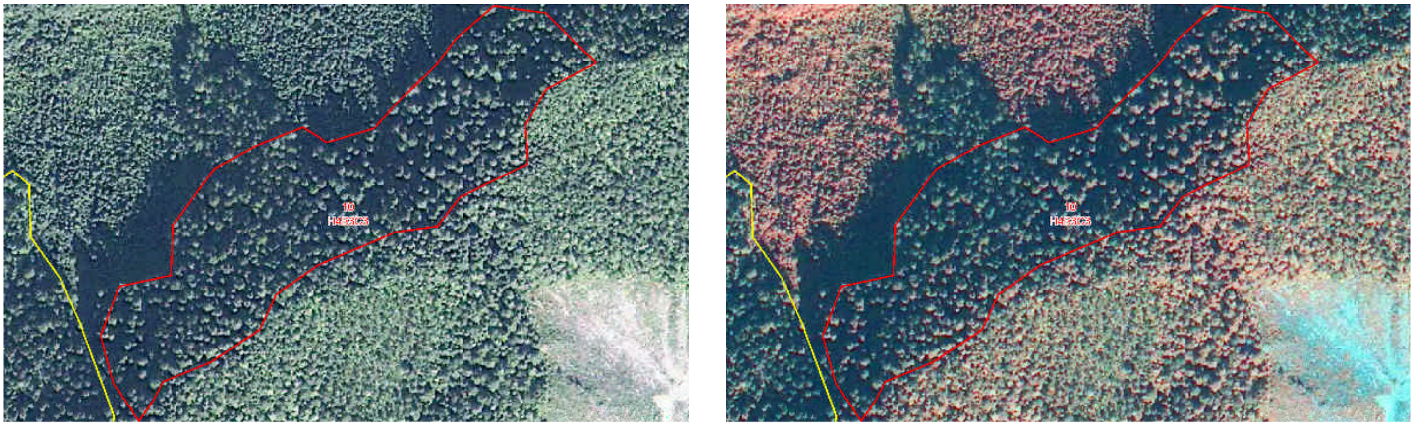

Figure 33. Polygon 10. RGB: Similar stand to polygon 7 with deep shadowing and less distinct shadows cast on lower slope. NIR: Distinct red colour signature to adjacent regeneration. © GeoEye

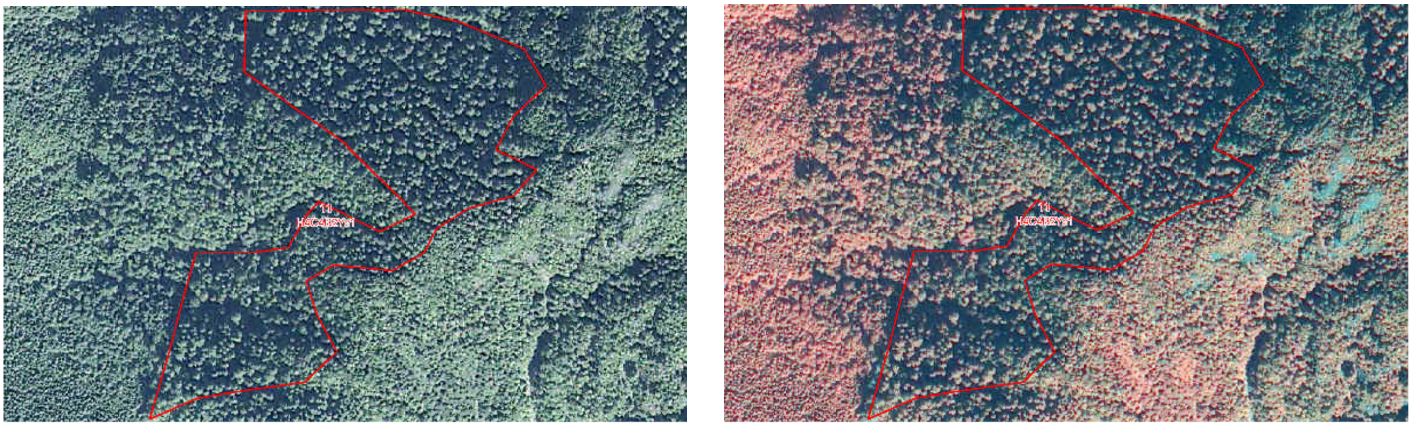

Figure 34. Polygon 11. RGB: Medium productivity stand with three major species. Tops of crowns easily seen but lower crowns in deep shadow. NIR: Adjacent regeneration areas and rock outcrops are well-defined. © GeoEye

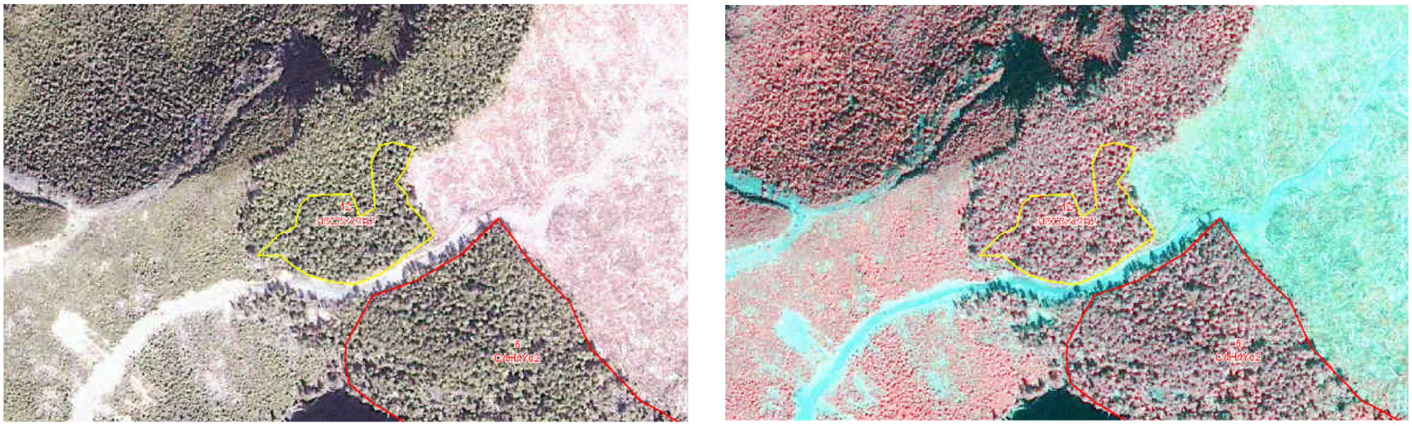

Figure 35. Polygon 12. RGB: Similar stand to polygon 6 with balsam component. Image is less distinct and more brownish in tone. NIR: Adjacent regeneration areas and rock outcrops are well-defined. © GeoEye

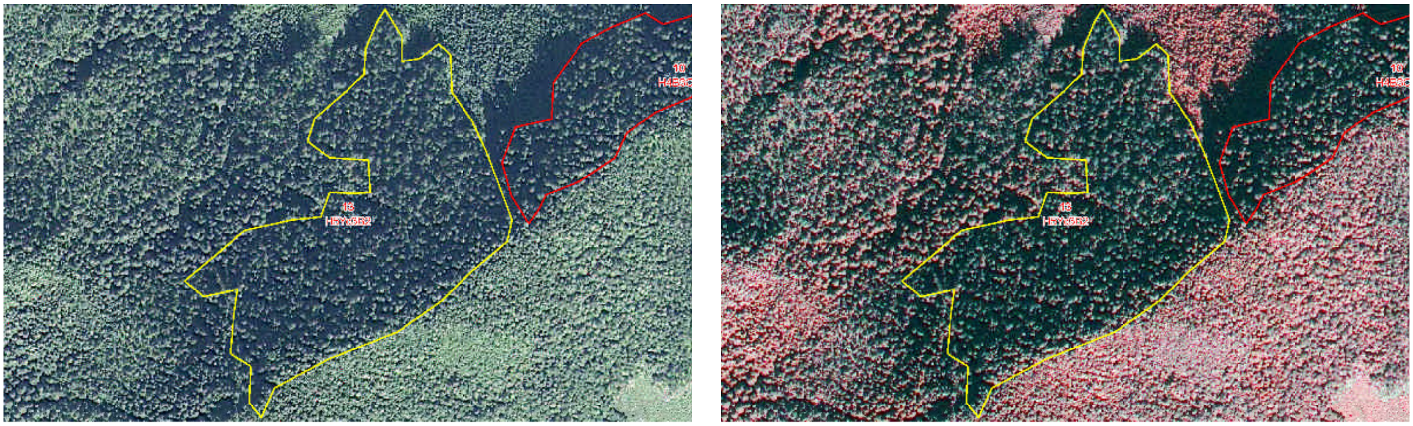

Figure 36. Polygon 13. RGB: Similar stand characteristics to polygon 10 but with some cypress. NIR: Adjacent regeneration areas well-defined. © GeoEye

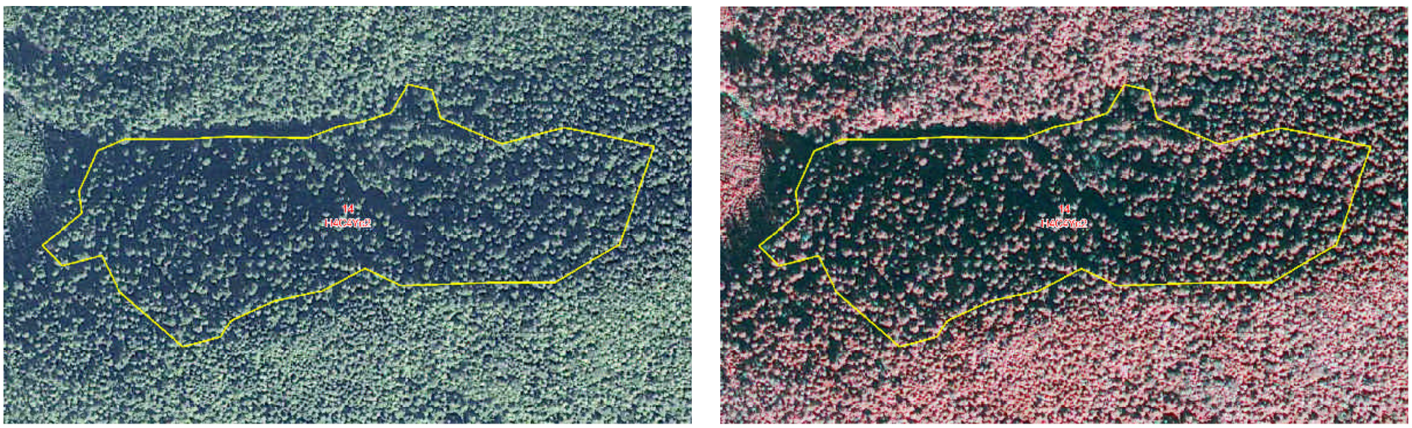

Figure 37. Polygon 14. RGB: Same comments as for polygon 11. NIR: Same comments as for polygon 13. © GeoEye

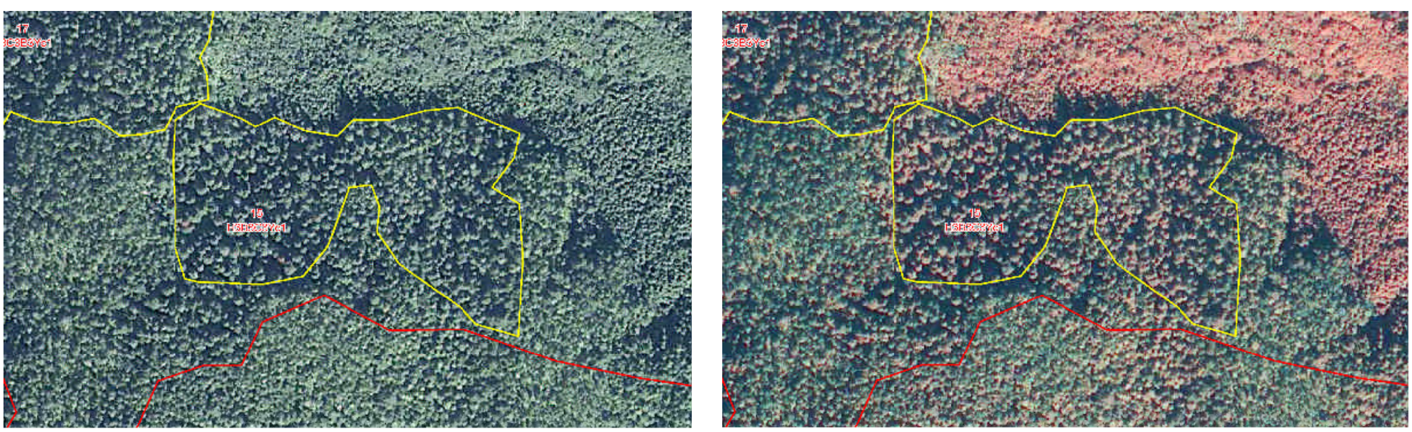

Figure 38. Polygon 15. RGB: Medium productivity stand with three major species. Tops of crowns easily seen but lower crowns in moderate shadow. Species identification aided by crown shadows. NIR: Adjacent regeneration areas well-defined. © GeoEye

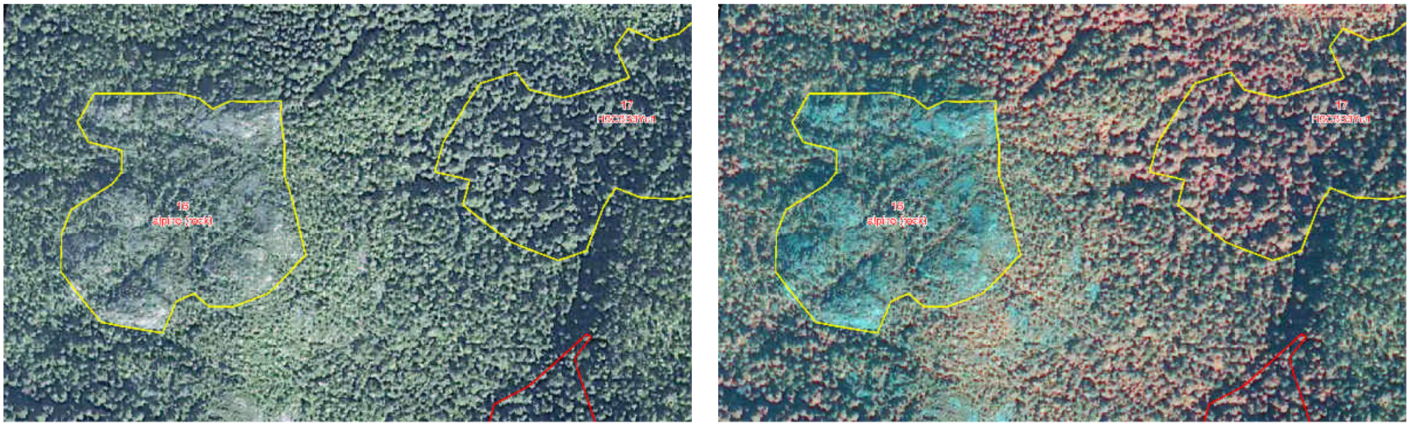

Figure 39. Polygon 16. RGB: Sparsely vegetated alpine area. NIR: NIR highlights rock outcrops. © GeoEye

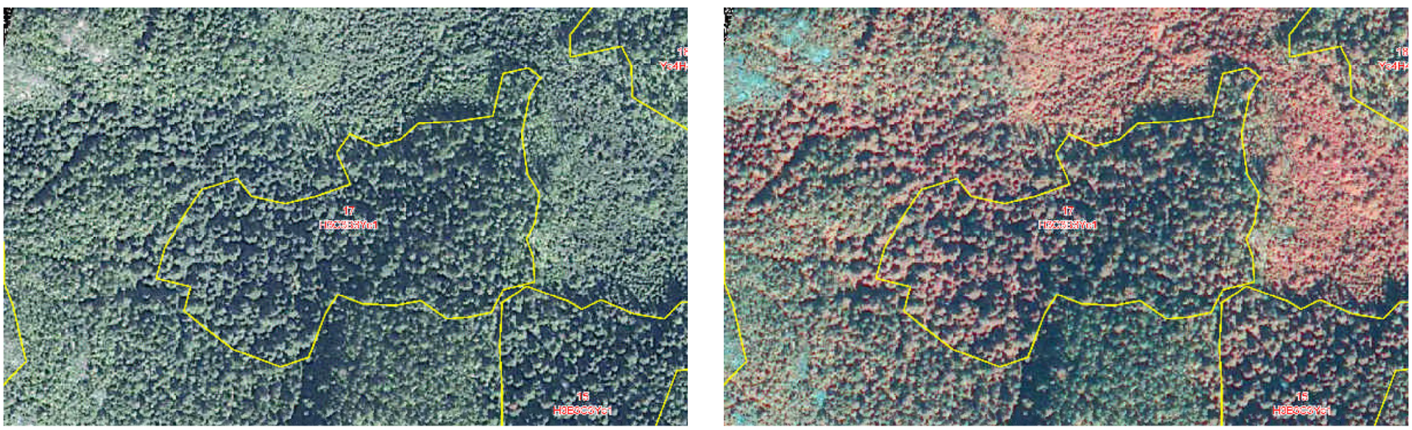

Figure 40. Polygon 17. RGB: Medium productivity stand with three major species. Tops of crowns easily seen but lower crowns in deep shadow. NIR: Adjacent regeneration areas well-defined. © GeoEye

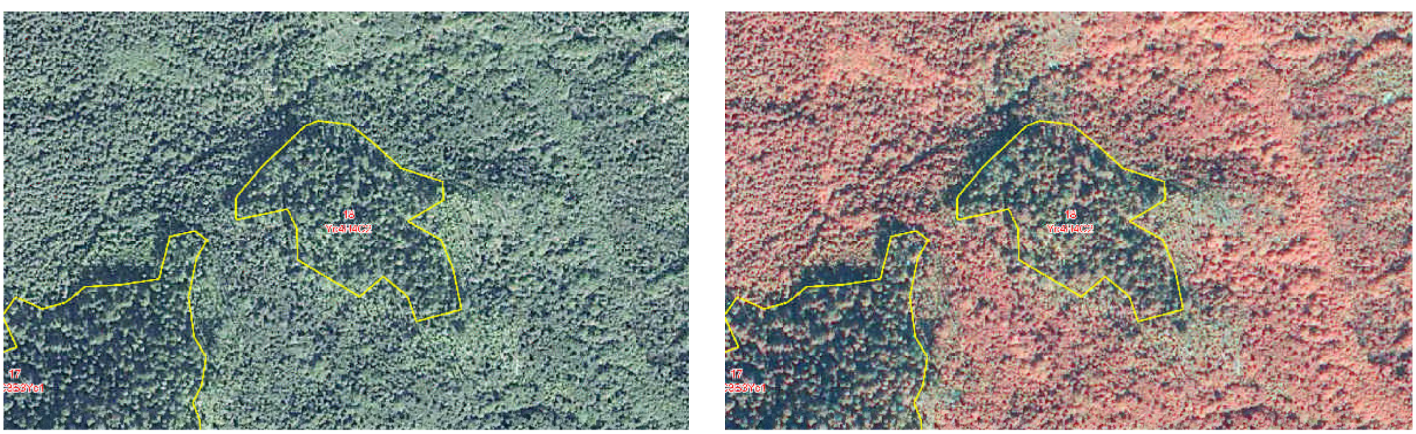

Figure 41. Polygon 18. RGB: Cypress/hemlock stand on rocky crest surrounded by young second growth. NIR: Highlights the isolated nature of these older trees surrounded by regeneration. © GeoEye

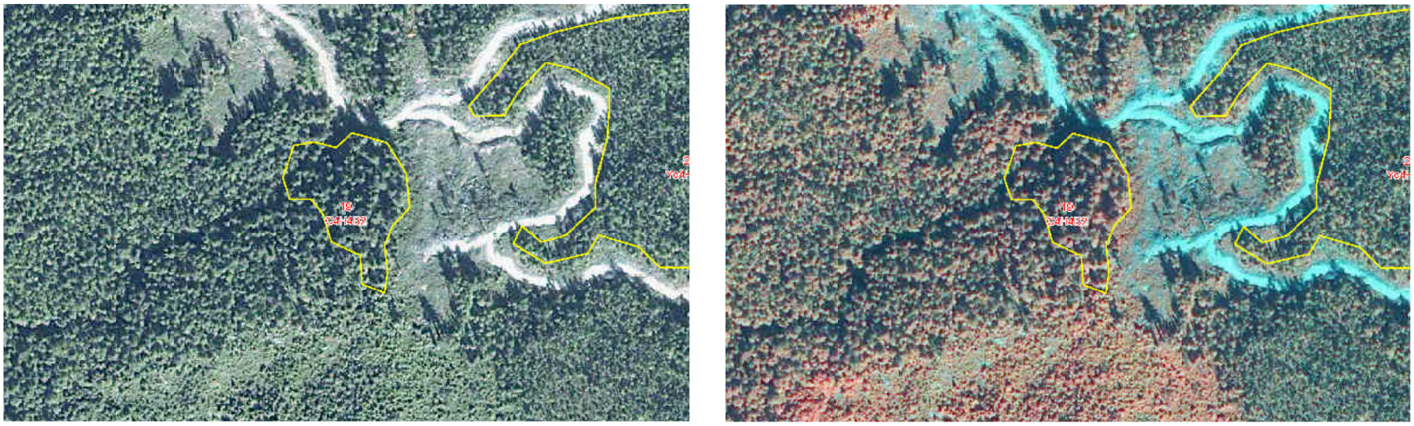

Figure 42. Polygon 19. RGB: Deep shadows within stand makes it hard to see crown shapes. Note adjacent recent cut block with reserve patches and scattered single trees. NIR: No additional interpretative assistance.© GeoEye

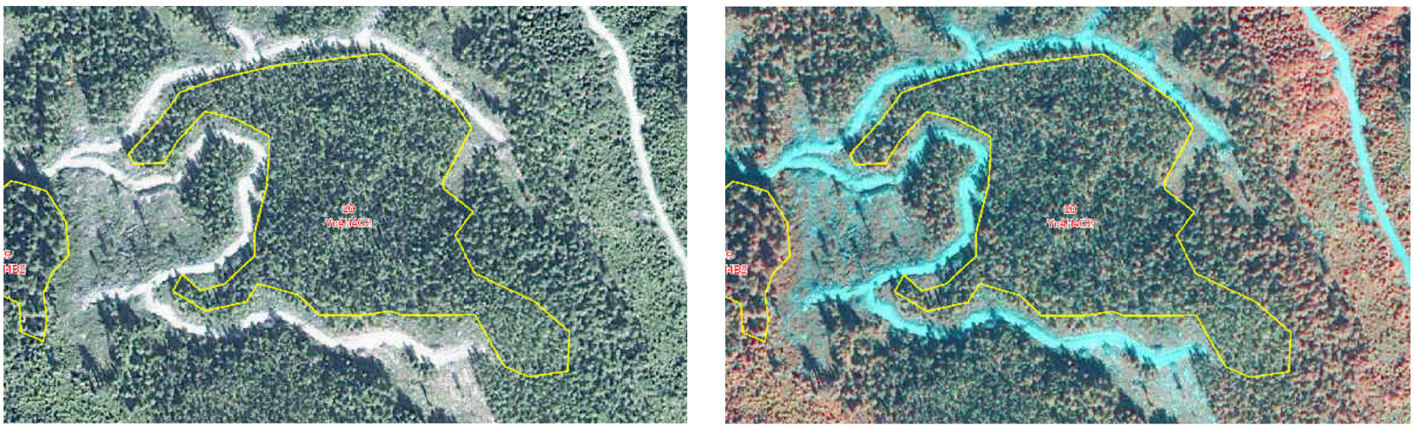

Figure 43. Polygon 20. RGB: Cypress leading low site, probably poorly drained. NIR: No additional interpretative assistance. © GeoEye

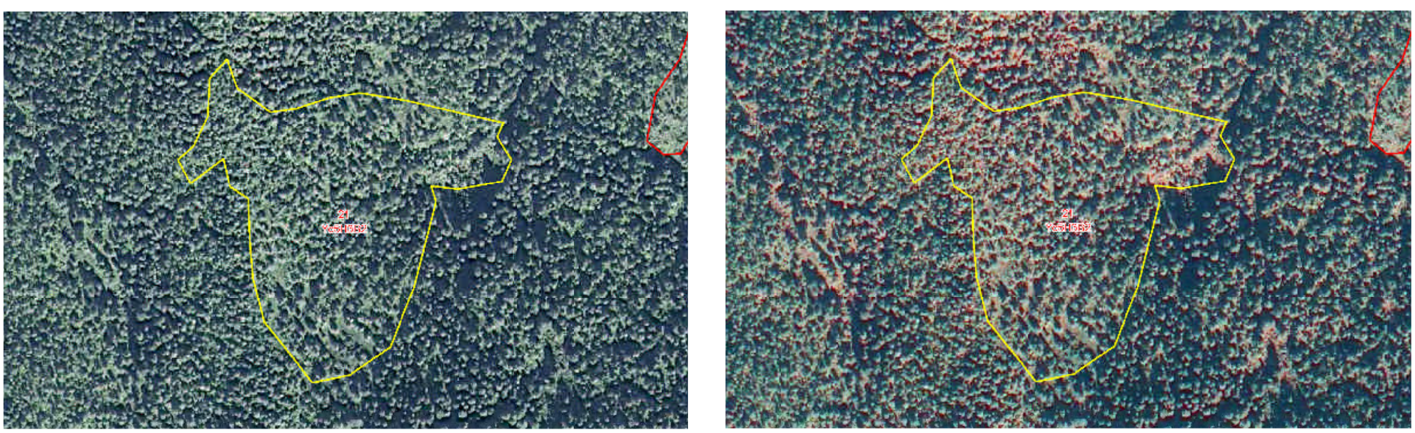

Figure 44. Polygon 21. RGB: Cypress dominated subalpine parkland forest. NIR: Open ground more evident with NIR. © GeoEye

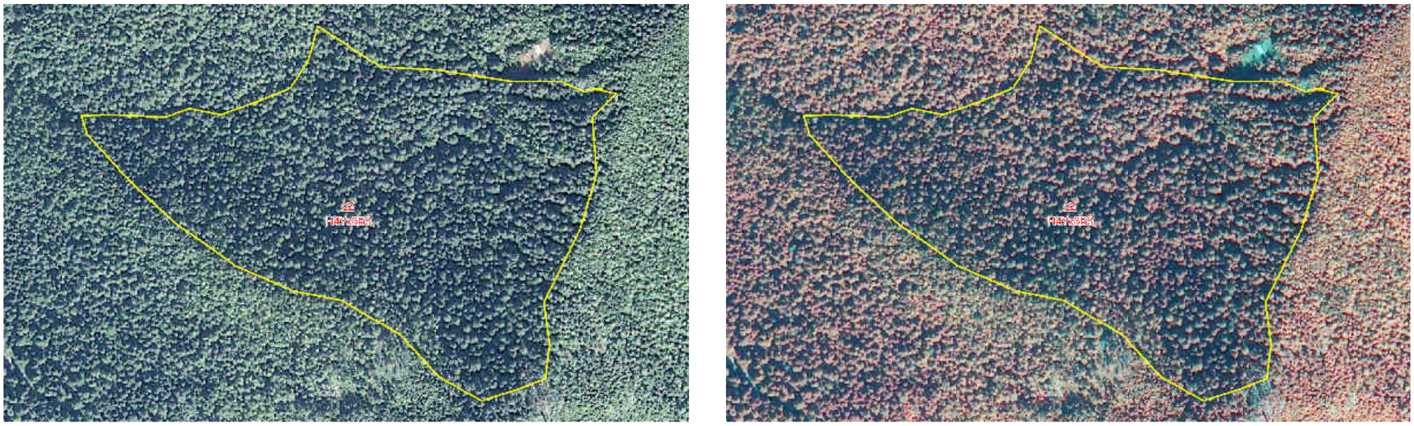

Figure 45. Polygon 22. RGB: High elevation productive hemlock/cypress/balsam stand surrounded by poorer rocky sites with smaller trees. NIR: No additional interpretive value for this stand but emphasizes the exposed rock on surrounding sites. © GeoEye

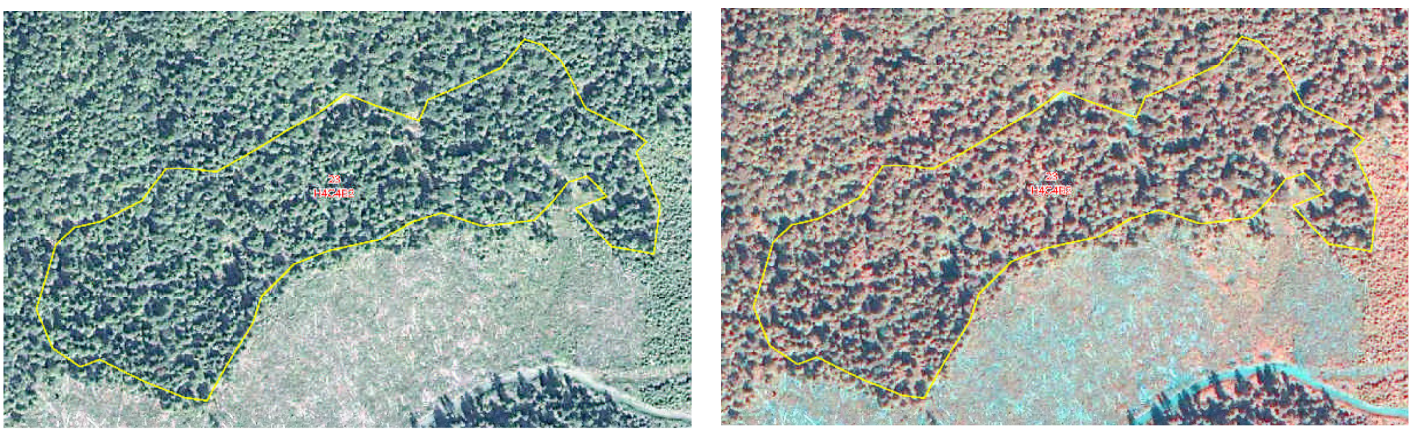

Figure 46. Polygon 23. RGB: Typical subalpine stand on thin soils with rock outcrops. Probably cypress rather than cedar is present in this stand. NIR: NIR highlights the openings in the stand due to rock outcrops. © GeoEye

3.0 CONCLUSIONS AND RECOMMENDATIONS

3.1 CONCLUSIONS

Reference Stereo IKONOS satellite images were acquired for August and October 2006, and were analyzed in stereo using softcopy photogrammetry. Various image colour composites were created and viewed in stereo and monoscopically. From our analysis of these images we have determined that summer imagery has more spectral variation than the fall imagery, possibly due to in part to more intense sunlight and variability in deciduous canopy, and provides the interpreter with a more interpretable image. There were also more, and longer, shadows in the October image, which made interpretation more difficult in the north facing slopes. Shadows were useful in helping to determine forest cover type.

The Reference Stereo IKONOS satellite imagery was easily loaded into the KLT softcopy photogrammetric workstation and referenced to ground coordinates using the supplied RPC files. Additional ground control from a hand-held GPS provided better positional accuracy. The hand-held GPS though is not as precise as a ground survey using a GPS with a base station, followed by post-processing in the office. Better positional accuracy could have been achieved with more precise GPS locations.

One limitation of the KLT softcopy photogrammetric workstation we encountered is that the RGB colour composite images required 8 bits per channel (24 bit all together), while the source IKONOS imagery has 11 bits per channel. We needed to compress the 11 bit data to 8 bits per channel, but were able to do this in a manner such that most of the spectral variation was kept, ie. data was compressed at the tails of the image histograms. This did not appear to hinder the image interpretation to a significant degree.

Forest Cover Analysis:

We compared a natural colour RGB, a false colour near-infrared, and a Principal Components colour composite image for interpretability of forest cover features. We have concluded

that an interpreter with forestry background, is more comfortable viewing the natural colour than the false colour near infrared image. Neither of these colour composite images was superior for all image interpretation. We recommend that both colour composite images be used for stereo viewing and interpretation.

Some general comments on the images by the interpreter:

- The August 2006 image shows tree species composition better than the October image which has less colour differentiation, deeper shadowing and is more "greyed out" overall;
- Textural changes due to differences in tree heights and species can be seen, especially when changes in terrain are also evident;
- Colour differences between various tree species are not easy to distinguish compared with hard copy air photos at a similar viewing scale. For example the usual yellowish colour signature of cedar and cypress crowns does not show up well;
- Distinguishing individual trees by species is not easy. Neither colour variation nor crown shapes is well-defined. There is insufficient depth in viewing the tree canopies and branching patterns;
- Some additional clues in interpreting species composition are gathered from shadows cast by tree crowns onto roads, open ground and water bodies. These shadows give a better view of the crown shapes than are visible within the stands;
- Use of the near-infrared channel does not help with species identification. In most cases, the tree crowns are fragmented into different colours/hues, and overall shape is less evident;
- Near-infrared does highlight age differences, especially between old growth trees on poor sites and regeneration/second growth on more productive sites. Non-vegetation features such as rock outcrops and exposed soil also stand out more;
- As with air photos, the spike tops on old growth cedars do not resolve on the image. When measuring these tree heights the "missing" tops must be accounted for;
- Generally, height measurements made on the image correlated quite well with both ocular estimates and attributes from the forest cover map, as long as the ground was visible. The more open the stand and the taller the trees, the easier it was to make accurate height measurements;
- Height measurements from the image did not correlate as well with map values where part of the original map polygon has been logged and the labels not adjusted to account for removal of the higher volume area of the stand.

Landscape Compilation:

Using the August satellite image, we compiled a terrain model for a section of the image. The area digitized was primarily heavily forested and had steep slopes. Spot heights and break lines were digitized, then rasterized to a consistent grid spacing Digital Elevation Model (DEM). A TRIM DEM covering the same area was compared with the IKONOS derived DEM. We determined that the elevations from the IKONOS derived DEM fit closely to the TRIM DEM elevations. The mean difference was 7.3m.

We also digitized an existing slide area in the image, capturing spot heights and break lines, to produce a DEM of the slide. We also created a theoretical pre-slide DEM and differenced the two DEMs to calculate the volume of material removed. We did not have any pre-slide data to confirm whether this area had a constant across-slope and down-slope curvature. It is possible that there was an existing drainage channel within the landslide area; if so, the actual volume of material should be smaller than we calculated.

Forest Practices Board Recommendations and Our Results:

The Forest Practices Board, FPB/SIR/14, July 2005, made several recommendations about managing landslide risk in BC. One of the recommendations was to use high spatial resolution, multispectral data, and stereoscopic viewing to improve the ability of a sensor for landslide detection. We are able to confirm that we can successfully map landslides in 3D using the Reference Stereo IKONOS imagery. The landslides were mapped using the natural colour RGB colour composite images. If we had pre-slide imagery for the same location, we would have been able to accurately calculate volume of material lost due to the slides. Due to IKONOS's large base height ratio (1 to 2), we had greater vertical exaggeration in the stereo image. This allowed the photogrammetric operator to more easily map steep slopes, and detect small variations in slope.

3.2 RECOMMENDATIONS

The availability of stereoscopic high spatial resolution imagery, and of image analysis software that allows for digitizing in 3D, greatly improves the efficiency of interpretation and identification of other geomorphic characteristics and the calculation of slope, elevation, landslide volumes and areas, and other features. Traditional film-based aerial photography requires coordinating with a firm to fly an area, getting the flying done, sending the film off for development, receiving the developed film and checking for scratches or other damage to the film, scanning the film, aerotriangulating the frames, and finally loading the frames into the softcopy photogrammetric workstation. Going the satellite route, the tasks are: ordering the digital imagery, receiving the imagery, and loading the imagery into the softcopy photogrammetric workstation. In short, the satellite route gets the operator to the stage of interpreting the imagery in stereo in less time than the aerial photo route.

If ground control is available, it can be applied to the satellite imagery to more closely relate it to ground coordinates. The same holds for the aerial photo route. From a cost/benefit perspective, high spatial resolution stereo satellite imagery is well-suited for mapping sites in remote areas, areas that are time sensitive, high priority forest crime areas, and areas that may be affected by insect infestation or other disease (as the near-infrared channel is sensitive to decrease in vegetation vigor caused by various stressors). The capability to select and manipulate the multi-spectral bands is an important feature that satellite imagery offers in contrast with standard aerial photography.

We used Reference Stereo IKONOS imagery for this project.

Table 7. Comparison of parameters of GeoEye-1 and Worldview-1 (DigitalGlobe) satellites.

	GeoEye-1	Worldview-1
Panchromatic spatial resolution at nadir / off nadir (Imagery for both satellites must be resampled to 50cm for non-US government users.)	42 cm at nadir. 50 cm out to 28° off-nadir.	45 cm at nadir. 51 cm out to 20° off-nadir.
Multispectral spatial resolution at nadir / off nadir	1.65 m at nadir. 1.96 m out to 28° off-nadir (author's calculation).	No multispectral sensor.
Swath width	15.2 km at nadir.	16 km at nadir.
Radiometric resolution	11 bits	11 bits
Temporal resolution	2.1 days at 59 cm pixel. 2.8 days at 50 cm pixel. 8.3 days at 42 cm pixel	1.7 days at 1m pixel or less. 5.9 days at 20° off-nadir or less for 51 cm pixel.
Positional accuracy	CE stereo 2m, LE stereo 3m, CE monoscopic 2.5m. These are specified as 90% CD for the horizontal and 90% LE for vertical with no ground control.	12.2m CE90, with predicted performance in the range of 3.0 to 7.6 meters CE90, excluding terrain and off-nadir effects.

As noted, this imagery has published positional accuracy of:

- 25m horizontal accuracy, and
- 22m vertical accuracy

at a 90% Confidence Level (CL).

One may want to consider if Precision Stereo IKONOS imagery can provide better mapping accuracy for forestry applications. The published positional accuracy for Precision Stereo IKONOS imagery is:

- 4m horizontal accuracy, and
- 5m vertical accuracy

at a 90% Confidence Level (CL).

The Precision Stereo IKONOS imagery does cost more than Reference Stereo imagery. For North America, the price for Precision Stereo is US$52.50 per sq km for panchromatic fused with colour imagery, with 100 sq km as the minimum order size. Reference Stereo imagery costs US$39.60 per sq km for panchromatic fused with colour imagery, with 100 sq km as the minimum order size.

GeoEye and DigitalGlobe both plan to launch new, higher spatial resolution satellites in 2007. The parameters of the two satellites are provided in Table 7.

It may be of interest to acquire stereo imagery when these new satellites are available. The lack of a multispectral sensor for Worldview 1 may make it less useful than the GeoEye-1 satellite imagery, which has a multispectral sensor.

4. 0 REFERENCES

Collins, D., Kliparchuk, K., Connor, M., Warttig, W. 2001. Preliminary assessment of the application of Ikonos satellite imagery and its fusion with Radarsat-1 data for forest resource management. Res. Sec., Van. For. Reg., B.C. Min. For., Nanaimo, B.C. Tec. Rep. TR-014/2001

Collins, D. and Kliparchuk, K, 2004. Forest resource change detection using high-resolution satellite imagery for monitoring and effectiveness evaluation. Res. Sec., Coast For. Reg., B.C. Min. For., Nanaimo, B.C. Tec. Rep. TR-030.

Kliparchuk, K. and Collins, D., 2003. Using QUICKBIRD sub-metre satellite imagery for implementation monitoring and effectiveness evaluation in forestry. Res. Sec., Vancouver For. Reg., B.C. Min. For., Nanaimo, B.C. Tec. Rep. TR-026.

Li, R., 1998. "Potential of High-Resolution Satellite Imagery for National Mapping Products". *In* Photogrammetric Engineering and Remote Sensing, Bethesda, Maryland, USA, Volume 64, Number 12, pp. 1165-1169.

Nichol, J.E., Shaker, A., Wong., M-S, 2006. Application of high-resolution stereo satellite images to detailed landslide hazard assessment. J. Geomorphology,76. pp 68-75

APPENDIX A: METADATA FOR AUGUST 2006 AND OCTOBER 2006 IMAGERY

Metadata for August 2006 imagery: po_200310_metadata.txt

Version Number: 1.5

Company Information
Address
GeoEye
12076 Grant Street
Thornton, Colorado 80241
U.S.A.
Contact Information
On the Web: http://www.geoeye.com
Customer Service Phone (U.S.A.): 1.800.232.9037
Customer Service Phone (World Wide): 1.703.480.7539
Customer Service Fax (World Wide): 1.703.450.9570
Customer Service Email: info@geoeye.com
Customer Service Center hours of operation:
Monday - Friday, 7:00-18:00 Eastern Standard Time

Product Order Metadata

Creation Date: 08/22/06
Product Work Order Number: 00116090
Product Order Number: 200310
Customer Project Name: Hesquiat, BC
Ground Station ID: PGS
License Type: Single Organization
License Option 1: 1 Company / Corporation: BC Ministry of Forests and Range
Product Order Area (Geographic Coordinates)
Number of Coordinates: 4
Coordinate: 1
Latitude: 49.5658100000 degrees
Longitude: -126.5543980000 degrees
Coordinate: 2
Latitude: 49.6007620000 degrees
Longitude: -126.4264440000 degrees
Coordinate: 3
Latitude: 49.5168650000 degrees
Longitude: -126.3766510000 degrees
Coordinate: 4
Latitude: 49.4836710000 degrees
Longitude: -126.5051940000 degrees
Sensor Type: Satellite
Sensor Name: IKONOS-2
Processing Level: Standard Geometrically Corrected
Image Type: PAN/MSI
Interpolation Method: Cubic Convolution
Multispectral Algorithm: Projective
Stereo: Stereo
Mosaic: No
Datum: WGS84
Product Order Pixel Size: 1.0000000000 meters
Product Order Map Units: meters
MTFC Applied: Yes
DRA Applied: No
Media: DVD
Product Media Format: DVD
File Format: TIFF
TIFF Tiled: No
Bits per Pixel per Band: 11 bits per pixel
Multispectral Files: Four Files

Source Image Metadata

Number of Source Images: 4

Source Image ID: 2006081619401110000011626609
Product Image ID: 000001
Sensor: IKONOS-2
Acquired Nominal GSD
Cross Scan: 0.87 meters
Along Scan: 0.92 meters
Scan Azimuth: 180.06 degrees
Scan Direction: Reverse
Panchromatic TDI Mode: 13
Nominal Collection Azimuth: 6.0060 degrees
Nominal Collection Elevation: 70.16835 degrees
Sun Angle Azimuth: 159.6433 degrees
Sun Angle Elevation: 52.75000 degrees
Acquisition Date/Time: 2006-08-16 19:40 GMT
Percent Cloud Cover: 19
Stereo Mate Image ID: 2006081619410310000011626610

Source Image ID: 2006081619410310000011626610
Product Image ID: 001000
Sensor: IKONOS-2
Acquired Nominal GSD
Cross Scan: 0.85 meters
Along Scan: 0.86 meters
Scan Azimuth: 180.06 degrees
Scan Direction: Reverse
Panchromatic TDI Mode: 13
Nominal Collection Azimuth: 209.7822 degrees
Nominal Collection Elevation: 76.96169 degrees
Sun Angle Azimuth: 159.9830 degrees
Sun Angle Elevation: 52.79884 degrees
Acquisition Date/Time: 2006-08-16 19:41 GMT
Percent Cloud Cover: 20
Stereo Mate Image ID: 2006081619401110000011626609

Source Image ID: 2006081619404470000011626608
Product Image ID: 002003

Sensor: IKONOS-2
Acquired Nominal GSD
Cross Scan: 0.82 meters
Along Scan: 0.82 meters
Scan Azimuth: 180.06 degrees
Scan Direction: Reverse
Panchromatic TDI Mode: 13
Nominal Collection Azimuth: 260.0834 degrees
Nominal Collection Elevation: 87.32711 degrees
Sun Angle Azimuth: 159.6475 degrees
Sun Angle Elevation: 52.75396 degrees
Acquisition Date/Time: 2006-08-16 19:40 GMT
Percent Cloud Cover: 31
Stereo Mate Image ID: 2006081619395360000011626607

Source Image ID: 2006081619395360000011626607
Product Image ID: 003002
Sensor: IKONOS-2
Acquired Nominal GSD
Cross Scan: 0.93 meters
Along Scan: 1.06 meters
Scan Azimuth: 180.06 degrees
Scan Direction: Reverse
Panchromatic TDI Mode: 13
Nominal Collection Azimuth: 10.7200 degrees
Nominal Collection Elevation: 60.72477 degrees
Sun Angle Azimuth: 159.3144 degrees
Sun Angle Elevation: 52.70521 degrees
Acquisition Date/Time: 2006-08-16 19:39 GMT
Percent Cloud Cover: 27
Stereo Mate Image ID: 2006081619404470000011626608

==

Product Space Metadata

Number of Image Components: 3
X Components: 2
Y Components: 1
Reference Height: 323.4087219238 meters

==

Product Component Metadata

Number of Components: 6

Component ID: 0000010000
Product Image ID: 000001
Component File Name: po_200310_red_0000010000.tif
po_200310_grn_0000010000.tif
po_200310_blu_0000010000.tif
po_200310_nir_0000010000.tif
Thumbnail File Name: po_200310_rgb_0000010000_ovr.jpg
Country Code: CA
Component Geographic Corner Coordinates
Number of Coordinates: 4
Coordinate: 1
Latitude: 49.5144018865 degrees
Longitude: -126.4738201737 degrees
Coordinate: 2
Latitude: 49.6068782602 degrees
Longitude: -126.4351842057 degrees
Coordinate: 3
Latitude: 49.5909485798 degrees
Longitude: -126.3453058009 degrees
Coordinate: 4
Latitude: 49.4985019917 degrees
Longitude: -126.3840986999 degrees
Percent Component Cloud Cover: 25
Stereo Position: Right
Stereo Mate File Name: po_200310_red_0010000000.tif
po_200310_grn_0010000000.tif
po_200310_blu_0010000000.tif
po_200310_nir_0010000000.tif

Component ID: 0010000000
Product Image ID: 001000
Component File Name: po_200310_red_0010000000.tif
po_200310_grn_0010000000.tif
po_200310_blu_0010000000.tif
po_200310_nir_0010000000.tif
Thumbnail File Name: po_200310_rgb_0010000000_ovr.jpg
Country Code: CA
Component Geographic Corner Coordinates
Number of Coordinates: 4
Coordinate: 1
Latitude: 49.5144018865 degrees
Longitude: -126.4738201737 degrees
Coordinate: 2
Latitude: 49.6068782602 degrees
Longitude: -126.4351842057 degrees
Coordinate: 3
Latitude: 49.5909485798 degrees
Longitude: -126.3453058009 degrees
Coordinate: 4
Latitude: 49.4985019917 degrees
Longitude: -126.3840986999 degrees
Percent Component Cloud Cover: 24
Stereo Position: Left
Stereo Mate File Name: po_200310_red_0000010000.tif
po_200310_grn_0000010000.tif
po_200310_blu_0000010000.tif
po_200310_nir_0000010000.tif

Component ID: 0020030000
Product Image ID: 002003
Component File Name: po_200310_red_0020030000.tif
po_200310_grn_0020030000.tif
po_200310_blu_0020030000.tif
po_200310_nir_0020030000.tif

Thumbnail File Name: po_200310_rgb_0020030000_ovr.jpg
Country Code: CA
Component Geographic Corner Coordinates
Number of Coordinates: 4
Coordinate: 1
Latitude: 49.4971467631 degrees
Longitude: -126.5825595268 degrees
Coordinate: 2
Latitude: 49.5958832057 degrees
Longitude: -126.5420328764 degrees
Coordinate: 3
Latitude: 49.5755404275 degrees
Longitude: -126.4253628520 degrees
Coordinate: 4
Latitude: 49.4768445651 degrees
Longitude: -126.4661074274 degrees
Percent Component Cloud Cover: 19
Stereo Position: Left
Stereo Mate File Name: po_200310_red_0030020000.tif
po_200310_grn_0030020000.tif
po_200310_blu_0030020000.tif
po_200310_nir_0030020000.tif

Component ID: 0020030100
Product Image ID: 002003
Component File Name: po_200310_red_0020030100.tif
po_200310_grn_0020030100.tif
po_200310_blu_0020030100.tif
po_200310_nir_0020030100.tif
Thumbnail File Name: po_200310_rgb_0020030100_ovr.jpg
Country Code: CA
Component Geographic Corner Coordinates
Number of Coordinates: 4
Coordinate: 1
Latitude: 49.5057043546 degrees
Longitude: -126.5152083358 degrees
Coordinate: 2
Latitude: 49.6088651096 degrees
Longitude: -126.4727210205 degrees
Coordinate: 3
Latitude: 49.5904096772 degrees
Longitude: -126.3671553992 degrees
Coordinate: 4
Latitude: 49.4872874041 degrees
Longitude: -126.4098487253 degrees
Percent Component Cloud Cover: 3
Stereo Position: Left
Stereo Mate File Name: po_200310_red_0030020100.tif
po_200310_grn_0030020100.tif
po_200310_blu_0030020100.tif
po_200310_nir_0030020100.tif

Component ID: 0030020000
Product Image ID: 003002
Component File Name: po_200310_red_0030020000.tif
po_200310_grn_0030020000.tif
po_200310_blu_0030020000.tif
po_200310_nir_0030020000.tif
Thumbnail File Name: po_200310_rgb_0030020000_ovr.jpg
Country Code: CA
Component Geographic Corner Coordinates
Number of Coordinates: 4
Coordinate: 1
Latitude: 49.4971467631 degrees
Longitude: -126.5825595268 degrees
Coordinate: 2
Latitude: 49.5958832057 degrees
Longitude: -126.5420328764 degrees
Coordinate: 3
Latitude: 49.5755404275 degrees
Longitude: -126.4253628520 degrees
Coordinate: 4
Latitude: 49.4768445651 degrees
Longitude: -126.4661074274 degrees
Percent Component Cloud Cover: 18
Stereo Position: Right
Stereo Mate File Name: po_200310_red_0020030000.tif
po_200310_grn_0020030000.tif
po_200310_blu_0020030000.tif
po_200310_nir_0020030000.tif

Component ID: 0030020100
Product Image ID: 003002
Component File Name: po_200310_red_0030020100.tif
po_200310_grn_0030020100.tif
po_200310_blu_0030020100.tif
po_200310_nir_0030020100.tif
Thumbnail File Name: po_200310_rgb_0030020100_ovr.jpg
Country Code: CA
Component Geographic Corner Coordinates
Number of Coordinates: 4
Coordinate: 1
Latitude: 49.5057043546 degrees
Longitude: -126.5152083358 degrees
Coordinate: 2
Latitude: 49.6088651096 degrees
Longitude: -126.4727210205 degrees
Coordinate: 3
Latitude: 49.5904096772 degrees
Longitude: -126.3671553992 degrees
Coordinate: 4
Latitude: 49.4872874041 degrees
Longitude: -126.4098487253 degrees
Percent Component Cloud Cover: 3
Stereo Position: Right
Stereo Mate File Name: po_200310_red_0020030100.tif
po_200310_grn_0020030100.tif
po_200310_blu_0020030100.tif
po_200310_nir_0020030100.tif

===

Metadata for October 2006 imagery: po_205758_metadata.txt

==

Version Number: 1.5

==

Company Information
Address
GeoEye
12076 Grant Street
Thornton, Colorado 80241
U.S.A.
Contact Information
On the Web: http://www.geoeye.com
Customer Service Phone (U.S.A.): 1.800.232.9037
Customer Service Phone (World Wide): 1.703.480.7539
Customer Service Fax (World Wide): 1.703.450.9570
Customer Service Email: info@geoeye.com
Customer Service Center hours of operation:
Monday - Friday, 7:00-18:00 Eastern Standard Time

==

Product Order Metadata

Creation Date: 10/12/06
Product Work Order Number: 00119963
Product Order Number: 205758
Customer Project Name: Hesquiat, BC
Ground Station ID: PGS
License Type: Single Organization
License Option 1: 1 Company / Corporation: BC Ministry of Forests and Range
Product Order Area (Geographic Coordinates)
Number of Coordinates: 4
Coordinate: 1
Latitude: 49.5658100000 degrees
Longitude: -126.5543980000 degrees
Coordinate: 2
Latitude: 49.6007620000 degrees
Longitude: -126.4264440000 degrees
Coordinate: 3
Latitude: 49.5168650000 degrees
Longitude: -126.3766510000 degrees
Coordinate: 4
Latitude: 49.4836710000 degrees
Longitude: -126.5051940000 degrees
Sensor Type: Satellite
Sensor Name: IKONOS-2
Processing Level: Standard Geometrically Corrected
Image Type: PAN/MSI
Interpolation Method: Cubic Convolution
Multispectral Algorithm: Projective
Stereo: Stereo
Mosaic: No
Datum: WGS84
Product Order Pixel Size: 1.0000000000 meters
Product Order Map Units: meters
MTFC Applied: Yes
DRA Applied: No
Media: DVD
Product Media Format: DVD
File Format: TIFF
TIFF Tiled: No
Bits per Pixel per Band: 11 bits per pixel
Multispectral Files: Four Files

==

Source Image Metadata

Number of Source Images: 4

Source Image ID: 2006101019440730000011606841
Product Image ID: 000001
Sensor: IKONOS-2
Acquired Nominal GSD
Cross Scan: 0.85 meters
Along Scan: 0.84 meters
Scan Azimuth: 180.06 degrees
Scan Direction: Reverse
Panchromatic TDI Mode: 13
Nominal Collection Azimuth: 250.4652 degrees
Nominal Collection Elevation: 79.11512 degrees
Sun Angle Azimuth: 171.4268 degrees
Sun Angle Elevation: 33.43938 degrees
Acquisition Date/Time: 2006-10-10 19:44 GMT
Percent Cloud Cover: 0
Stereo Mate Image ID: 2006101019431730000011606840

Source Image ID: 2006101019431730000011606840
Product Image ID: 001000
Sensor: IKONOS-2
Acquired Nominal GSD
Cross Scan: 0.90 meters
Along Scan: 1.00 meters
Scan Azimuth: 180.06 degrees
Scan Direction: Reverse
Panchromatic TDI Mode: 13
Nominal Collection Azimuth: 356.5362 degrees
Nominal Collection Elevation: 64.52547 degrees
Sun Angle Azimuth: 171.1795 degrees
Sun Angle Elevation: 33.41880 degrees
Acquisition Date/Time: 2006-10-10 19:43 GMT
Percent Cloud Cover: 2
Stereo Mate Image ID: 2006101019440730000011606841

Source Image ID: 2006101019442890000011606839
Product Image ID: 002003
Sensor: IKONOS-2
Acquired Nominal GSD
Cross Scan: 0.90 meters

Along Scan: 0.91 meters
Scan Azimuth: 180.06 degrees
Scan Direction: Reverse
Panchromatic TDI Mode: 13
Nominal Collection Azimuth: 217.9358 degrees
Nominal Collection Elevation: 69.24263 degrees
Sun Angle Azimuth: 171.3696 degrees
Sun Angle Elevation: 33.43731 degrees
Acquisition Date/Time: 2006-10-10 19:44 GMT
Percent Cloud Cover: 0
Stereo Mate Image ID: 2006101019433970000011606838

Source Image ID: 2006101019433970000011606838
Product Image ID: 003002
Sensor: IKONOS-2
Acquired Nominal GSD
Cross Scan: 0.85 meters
Along Scan: 0.87 meters
Scan Azimuth: 180.06 degrees
Scan Direction: Reverse
Panchromatic TDI Mode: 13
Nominal Collection Azimuth: 340.0991 degrees
Nominal Collection Elevation: 76.43000 degrees
Sun Angle Azimuth: 171.1263 degrees
Sun Angle Elevation: 33.41693 degrees
Acquisition Date/Time: 2006-10-10 19:43 GMT
Percent Cloud Cover: 0
Stereo Mate Image ID: 2006101019442890000011606839

==

Product Space Metadata

Number of Image Components: 3
X Components: 2
Y Components: 1
Reference Height: 323.4087219238 meters

==

Product Component Metadata

Number of Components: 6

Component ID: 0000010000
Product Image ID: 000001
Component File Name: po_205758_red_0000010000.tif
po_205758_grn_0000010000.tif
po_205758_blu_0000010000.tif
po_205758_nir_0000010000.tif
Thumbnail File Name: po_205758_rgb_0000010000_ovr.jpg
Country Code: CA
Component Geographic Corner Coordinates
Number of Coordinates: 4
Coordinate: 1
Latitude: 49.5122688426 degrees
Longitude: -126.4548553210 degrees
Coordinate: 2
Latitude: 49.5986034887 degrees
Longitude: -126.4175486771 degrees
Coordinate: 3
Latitude: 49.5848470591 degrees
Longitude: -126.3424861515 degrees
Coordinate: 4
Latitude: 49.4985364253 degrees
Longitude: -126.3799144685 degrees
Percent Component Cloud Cover: 0
Stereo Position: Left
Stereo Mate File Name: po_205758_red_0010000000.tif
po_205758_grn_0010000000.tif
po_205758_blu_0010000000.tif
po_205758_nir_0010000000.tif

Component ID: 0010000000
Product Image ID: 001000
Component File Name: po_205758_red_0010000000.tif
po_205758_grn_0010000000.tif
po_205758_blu_0010000000.tif
po_205758_nir_0010000000.tif
Thumbnail File Name: po_205758_rgb_0010000000_ovr.jpg
Country Code: CA
Component Geographic Corner Coordinates
Number of Coordinates: 4
Coordinate: 1
Latitude: 49.5122688426 degrees
Longitude: -126.4548553210 degrees
Coordinate: 2
Latitude: 49.5986034887 degrees
Longitude: -126.4175486771 degrees
Coordinate: 3
Latitude: 49.5848470591 degrees
Longitude: -126.3424861515 degrees
Coordinate: 4
Latitude: 49.4985364253 degrees
Longitude: -126.3799144685 degrees
Percent Component Cloud Cover: 8
Stereo Position: Right
Stereo Mate File Name: po_205758_red_0000010000.tif
po_205758_grn_0000010000.tif
po_205758_blu_0000010000.tif
po_205758_nir_0000010000.tif

Component ID: 0020030000
Product Image ID: 002003
Component File Name: po_205758_red_0020030000.tif
po_205758_grn_0020030000.tif
po_205758_blu_0020030000.tif
po_205758_nir_0020030000.tif
Thumbnail File Name: po_205758_rgb_0020030000_ovr.jpg
Country Code: CA
Component Geographic Corner Coordinates

Number of Coordinates: 4
Coordinate: 1
Latitude: 49.4983628428 degrees
Longitude: -126.5840068486 degrees
Coordinate: 2
Latitude: 49.5964165927 degrees
Longitude: -126.5409286265 degrees
Coordinate: 3
Latitude: 49.5745035158 degrees
Longitude: -126.4234945440 degrees
Coordinate: 4
Latitude: 49.4764931765 degrees
Longitude: -126.4667881554 degrees
Percent Component Cloud Cover: 0
Stereo Position: Left
Stereo Mate File Name: po_205758_red_0030020000.tif
po_205758_grn_0030020000.tif
po_205758_blu_0030020000.tif
po_205758_nir_0030020000.tif

Component ID: 0020030100
Product Image ID: 002003
Component File Name: po_205758_red_0020030100.tif
po_205758_grn_0020030100.tif
po_205758_blu_0020030100.tif
po_205758_nir_0020030100.tif
Thumbnail File Name: po_205758_rgb_0020030100_ovr.jpg
Country Code: CA
Component Geographic Corner Coordinates
Number of Coordinates: 4
Coordinate: 1
Latitude: 49.5067540225 degrees
Longitude: -126.5170619425 degrees
Coordinate: 2
Latitude: 49.6092747114 degrees
Longitude: -126.4718539673 degrees
Coordinate: 3
Latitude: 49.5889067856 degrees
Longitude: -126.3630311856 degrees
Coordinate: 4
Latitude: 49.4864283028 degrees
Longitude: -126.4084478089 degrees
Percent Component Cloud Cover: 0
Stereo Position: Left
Stereo Mate File Name: po_205758_red_0030020100.tif
po_205758_grn_0030020100.tif
po_205758_blu_0030020100.tif
po_205758_nir_0030020100.tif

Component ID: 0030020000
Product Image ID: 003002
Component File Name: po_205758_red_0030020000.tif
po_205758_grn_0030020000.tif
po_205758_blu_0030020000.tif
po_205758_nir_0030020000.tif
Thumbnail File Name: po_205758_rgb_0030020000_ovr.jpg
Country Code: CA
Component Geographic Corner Coordinates
Number of Coordinates: 4
Coordinate: 1
Latitude: 49.4983628428 degrees
Longitude: -126.5840068486 degrees
Coordinate: 2
Latitude: 49.5964165927 degrees
Longitude: -126.5409286265 degrees
Coordinate: 3
Latitude: 49.5745035158 degrees
Longitude: -126.4234945440 degrees
Coordinate: 4
Latitude: 49.4764931765 degrees
Longitude: -126.4667881554 degrees
Percent Component Cloud Cover: 0
Stereo Position: Right
Stereo Mate File Name: po_205758_red_0020030000.tif
po_205758_grn_0020030000.tif
po_205758_blu_0020030000.tif
po_205758_nir_0020030000.tif

Component ID: 0030020100
Product Image ID: 003002
Component File Name: po_205758_red_0030020100.tif
po_205758_grn_0030020100.tif
po_205758_blu_0030020100.tif
po_205758_nir_0030020100.tif
Thumbnail File Name: po_205758_rgb_0030020100_ovr.jpg
Country Code: CA
Component Geographic Corner Coordinates
Number of Coordinates: 4
Coordinate: 1
Latitude: 49.5067540225 degrees
Longitude: -126.5170619425 degrees
Coordinate: 2
Latitude: 49.6092747114 degrees
Longitude: -126.4718539673 degrees
Coordinate: 3
Latitude: 49.5889067856 degrees
Longitude: -126.3630311856 degrees
Coordinate: 4
Latitude: 49.4864283028 degrees
Longitude: -126.4084478089 degrees
Percent Component Cloud Cover: 1
Stereo Position: Right
Stereo Mate File Name: po_205758_red_0020030100.tif
po_205758_grn_0020030100.tif
po_205758_blu_0020030100.tif
po_205758_nir_0020030100.tif

==

APPENDIX B: RPC BUNDLE ADJUSTMENT

by ProjectLT v1.14.019[x64]
Scene#1: 200310_RGB_0030020000
Scene#2: 200310_RGB_0020030000
(Ground) Residuals on Tie Points (RPCs v. RPCs+TiePoints)

				Unadjusted RPCs		RPCs+Tie Points	
	Gnd			Gnd		Gnd	
Pnt#	GX	GY	GZ	RAWVX	RAWVY	ADJ1VX	ADJ1VY
01	681428.309	5485346.828	287.104	-0.493	0.118	-0.372	0.089
10	678108.132	5490558.129	23.456	0.780	-0.184	0.883	-0.209
13	682225.677	5495083.749	703.984	0.681	-0.155	-1.531	0.361
15	685470.290	5491898.335	586.320	1.119	-0.261	-1.482	0.345
02	683814.484	5486464.809	564.128	-0.004	0.001	-0.906	0.211
03	680900.261	5487203.394	142.640	-1.897	0.445	-1.999	0.468
07	683356.743	5489618.865	480.320	1.501	-0.350	0.079	-0.019
08	683516.665	5489925.580	684.800	6.866	-1.605	5.328	-1.247
			RMS:	2.635	0.616	2.199	0.515

(Ground) Residuals on Survey Check Points
Pnt# | GVX GVY GVZ
** No Check Points in GROUND.CHK File: GROUND.CHK

(Ground) Residuals on Survey Control Points

Pnt#	GVX	GVY	GVZ
01	0.461	4.611	-2.423
10	-1.005	-7.906	2.332
13	-7.836	6.330	-3.904
15	8.488	-2.323	9.814
02	-1.729	0.471	-7.138
03	0.288	-0.871	2.071
07	0.350	-9.584	-3.135
08	0.983	9.272	2.383
RMS:	4.166	6.205	4.920

(Pixel) Residuals on Survey Control Points

Pnt#	Scene#1		Scene#2	
01	0.78	-2.53	-1.64	-2.55
10	0.35	3.20	4.04	3.55
13	-0.63	4.06	10.11	0.94
15	-14.09	1.48	-8.33	-1.06
02	7.27	-2.93	4.94	-3.77
03	-1.80	2.25	-0.87	0.22
07	4.42	-0.76	8.03	-1.20
08	-8.46	-2.91	-4.14	1.98
RMS:	6.58	2.69	6.10	2.26

Scene#1: 200310_RGB_0030020000
Scene#2: po_205758_RGB_0020030000
(Ground) Residuals on Tie Points (RPCs v. RPCs+TiePoints)

				Unadjusted RPCs		RPCs+Tie Points	
	Gnd			Gnd		Gnd	
Pnt#	GX	GY	GZ	RAWVX	RAWVY	ADJ1VX	ADJ1VY
01	681427.711	5485342.850	279.920	-0.478	0.170	1.879	-0.672
10	678109.523	5490557.592	23.312	-2.602	0.934	-0.120	0.042
13	682225.081	5495081.703	700.048	2.597	-0.930	0.503	-0.180
15	685469.339	5491894.250	578.560	0.991	-0.359	-1.996	0.714
02	683814.350	5486460.888	557.264	-0.650	0.228	-0.341	0.121
03	680902.049	5487199.669	137.520	-4.793	1.715	-2.831	1.013
07	683357.268	5489613.240	470.896	-2.988	1.069	-3.642	1.306
08	683513.927	5489921.360	675.504	7.428	-2.663	6.547	-2.345
			RMS:	3.574	1.281	3.001	1.075

(Ground) Residuals on Survey Check Points

Pnt#	GVX	GVY	GVZ

** No Check Points in GROUND.CHK File: GROUND.CHK

(Ground) Residuals on Survey Control Points

Pnt#	GVX	GVY	GVZ
01	-0.242	5.973	-2.989
10	0.448	-9.031	0.990
13	-10.745	5.207	-5.675
15	7.384	0.107	11.523
02	-2.026	0.437	-6.964
03	1.167	-0.060	0.914
07	0.575	-4.421	-3.916
08	3.441	1.789	6.118
RMS:	4.846	4.573	5.884

(Pixel) Residuals on Survey Control Points

Pnt#	Scene#1		Scene#2	
01	1.36	-3.73	-3.63	-0.84
10	0.71	1.91	7.42	0.58
13	-1.42	5.74	13.92	3.18
15	-15.08	3.37	-7.97	-0.76
02	7.36	-2.87	3.67	-2.65
03	-1.45	1.20	-0.84	-1.89
07	4.11	-0.18	5.63	-4.66
08	-8.77	-2.04	-4.99	3.84
RMS:	6.91	3.08	7.04	2.71

Scene#1: 200310_RGB_0030020000
Scene#2: po_205758_RGB_0030020000
(Ground) Residuals on Tie Points (RPCs v. RPCs+TiePoints)

				Unadjusted RPCs		RPCs+Tie Points	
	Gnd			Gnd		Gnd	
Pnt#	GX	GY	GZ	RAWVX	RAWVY	ADJ1VX	ADJ1VY
01	681426.084	5485342.636	278.160	1.683	-0.898	2.827	-1.505
10	678109.716	5490559.537	27.024	-2.172	1.156	-0.764	0.409
13	682225.792	5495086.020	707.792	2.666	-1.423	0.290	-0.155
15	685468.767	5491894.953	579.008	1.459	-0.778	-1.777	0.947
02	683814.628	5486461.144	558.080	-1.878	1.000	-2.457	1.310
03	680899.804	5487200.808	138.336	-3.202	1.698	-2.341	1.242
07	683356.348	5489614.160	471.952	-0.446	0.237	-1.753	0.934
08	683513.649	5489924.468	679.488	7.467	-3.978	5.974	-3.182
			RMS:	3.289	1.751	2.786	1.484

(Ground) Residuals on Survey Check Points

Pnt#	GVX	GVY	GVZ

** No Check Points in GROUND.CHK File: GROUND.CHK

(Ground) Residuals on Survey Control Points

Pnt#	GVX	GVY	GVZ
01	-0.705	8.000	-2.210
10	-0.633	-10.979	0.088
13	-9.484	7.729	-3.354
15	7.144	-0.457	10.454
02	0.063	-0.392	-7.056
03	1.039	-0.075	1.318
07	-0.161	-5.491	-3.764
08	2.738	1.666	4.525
RMS:	4.337	5.890	5.143

(Pixel) Residuals on Survey Control Points

Pnt#	Scene#1		Scene#2	
01	0.30	-3.69	-1.44	0.41
10	2.81	2.75	5.34	0.72
13	2.25	6.11	9.71	3.07
15	-13.67	2.83	-11.51	-1.06
02	6.43	-3.22	4.97	-5.52
03	-1.54	1.35	-1.78	-1.34
07	4.80	-0.36	5.16	-2.92
08	-7.90	-2.14	-3.89	3.13
RMS:	6.41	3.23	6.39	2.78